frontiers | Frontiers in Endocrinology

TYPE Original Research
PUBLISHED 31 July 2024
DOI 10.3389/fendo.2024.1440070

OPEN ACCESS

EDITED BY
Yuko Maejima,
Fukushima Medical University, Japan

REVIEWED BY
Yoichi Ueta,
University of Occupational and Environmental Health Japan, Japan
Taka-aki Koshimizu,
Jichi Medical University, Japan

*CORRESPONDENCE
James E. Blevins
jeblevin@uw.edu

RECEIVED 28 May 2024
ACCEPTED 28 June 2024
PUBLISHED 31 July 2024

CITATION
Edwards MM, Nguyen HK, Dodson AD, Herbertson AJ, Wolden-Hanson T, Wietecha TA, Honeycutt MK, Slattery JD, O'Brien KD, Graham JL, Havel PJ, Mundinger TO, Sikkema CL, Peskind ER, Ryu V, Taborsky GJ Jr. and Blevins JE (2024) Sympathetic innervation of interscapular brown adipose tissue is not a predominant mediator of oxytocin-elicited reductions of body weight and adiposity in male diet-induced obese mice.
Front. Endocrinol. 15:1440070.
doi: 10.3389/fendo.2024.1440070

Sympathetic innervation of interscapular brown adipose tissue is not a predominant mediator of oxytocin-elicited reductions of body weight and adiposity in male diet-induced obese mice

Melise M. Edwards[1], Ha K. Nguyen[1], Andrew D. Dodson[1], Adam J. Herbertson[1], Tami Wolden-Hanson[1], Tomasz A. Wietecha[2,3], Mackenzie K. Honeycutt[1], Jared D. Slattery[1], Kevin D. O'Brien[2,3], James L. Graham[4], Peter J. Havel[4,5], Thomas O. Mundinger[6], Carl L. Sikkema[1,7], Elaine R. Peskind[1,7], Vitaly Ryu[8], Gerald J. Taborsky Jr.[1,6] and James E. Blevins[1,6]*

[1]VA Puget Sound Health Care System, Office of Research and Development Medical Research Service, Department of Veterans Affairs Medical Center, Seattle, WA, United States, [2]Division of Cardiology, Department of Medicine, University of Washington School of Medicine, Seattle, WA, United States, [3]UW Medicine Diabetes Institute, University of Washington School of Medicine, Seattle, WA, United States, [4]Department of Nutrition, University of California, Davis, Davis, CA, United States, [5]Department of Molecular Biosciences, School of Veterinary Medicine, University of California, Davis, Davis, CA, United States, [6]Division of Metabolism, Endocrinology and Nutrition, Department of Medicine, University of Washington School of Medicine, Seattle, WA, United States, [7]Department of Psychiatry and Behavioral Sciences, University of Washington School of Medicine, Seattle, WA, United States, [8]Department of Medicine and Pharmacological Sciences, Icahn School of Medicine at Mount Sinai, New York, NY, United States

Previous studies indicate that CNS administration of oxytocin (OT) reduces body weight in high fat diet-induced obese (DIO) rodents by reducing food intake and increasing energy expenditure (EE). We recently demonstrated that hindbrain (fourth ventricular [4V]) administration of OT elicits weight loss and elevates interscapular brown adipose tissue temperature (T_{IBAT}, a surrogate measure of increased EE) in DIO mice. What remains unclear is whether OT-elicited weight loss requires increased sympathetic nervous system (SNS) outflow to IBAT. We hypothesized that OT-induced stimulation of SNS outflow to IBAT contributes to its ability to activate BAT and elicit weight loss in DIO mice. To test this hypothesis, we determined the effect of disrupting SNS activation of IBAT on the ability of 4V OT administration to increase T_{IBAT} and elicit weight loss in DIO mice. We first determined whether bilateral surgical SNS denervation to IBAT was successful as noted by ≥ 60% reduction in IBAT norepinephrine (NE) content in DIO mice. NE content was selectively reduced in IBAT at 1-, 6- and 7-weeks post-denervation by 95.9 ± 2.0, 77.4 ± 12.7 and 93.6 ± 4.6% ($P<0.05$), respectively and was unchanged in inguinal white adipose tissue, pancreas or liver. We subsequently measured the effects of acute 4V OT (1, 5 µg ≈ 0.99, 4.96 nmol)

10.3389/fendo.2024.1440070

on T_{IBAT} in DIO mice following sham or bilateral surgical SNS denervation to IBAT. We found that the high dose of 4V OT (5 μg ≈ 4.96 nmol) elevated T_{IBAT} similarly in sham mice as in denervated mice. We subsequently measured the effects of chronic 4V OT (16 nmol/day over 29 days) or vehicle infusions on body weight, adiposity and food intake in DIO mice following sham or bilateral surgical denervation of IBAT. Chronic 4V OT reduced body weight by 5.7 ± 2.23% and 6.6 ± 1.4% in sham and denervated mice ($P<0.05$), respectively, and this effect was similar between groups (P=NS). OT produced corresponding reductions in whole body fat mass ($P<0.05$). Together, these findings support the hypothesis that sympathetic innervation of IBAT is not necessary for OT-elicited increases in BAT thermogenesis and reductions of body weight and adiposity in male DIO mice.

KEYWORDS

obesity, brown adipose tissue (BAT), white adipose tissue (WAT), oxytocin, food intake

Introduction

While the hypothalamic neuropeptide, oxytocin (OT), has a more clearly established role in the control of reproductive behavior (1) and prosocial behavior (2, 3), it has also been recognized as having an important role in the control of food intake and body weight (4–7). Although OT reduces body weight in part by decreasing energy intake, pair-feeding studies indicate that OT-elicited reductions of weight gain or weight loss cannot be fully explained by its ability to decrease energy intake (8–10). In these studies, pair-feeding appears to account for approximately 50% of the reduction of weight gain and/or weight loss observed with OT treatment (8–10)

Indeed, recent studies have shown that OT increases energy expenditure (EE) (11–14). While brown adipose tissue thermogenesis (BAT) is important in the control of EE [for review see (15, 16)], it is unclear whether OT's effects on EE result primarily from 1) activation of non-shivering BAT thermogenesis, 2) spontaneous physical activity-induced thermogenesis (17), 3) shivering and non-shivering thermogenesis in skeletal muscle (18), or 4) endocrine factors [e.g. thyroid hormone, fibroblast growth factor-21, irisin (for review see (19, 20))]. We have found that acute third (3V) and fourth ventricular (4V) injections of OT increase interscapular BAT temperature (T_{IBAT}), a functional readout of BAT thermogenesis in mice and rats (21, 22). Furthermore, the effects of chronic CNS administration of OT on T_{IBAT} coincide with OT-elicited weight loss in diet-induced obese (DIO) rats (21). Sutton and colleagues demonstrated that use of designer drugs (DREADDs) technology to chemogenetically activate hypothalamic paraventricular nucleus (PVN) OT neurons increases both EE and tends to increase subcutaneous BAT temperature (P=0.13) in *Oxytocin-Ires-Cre* mice (23). Furthermore, Yuan et al. recently reported that peripheral administration of OT promotes BAT differentiation *in vitro* and the expression of genes involved in thermogenesis in IBAT in high fat diet-fed mice (24). On the other hand, reduced OT signaling is associated with obesity (14, 25–27), reductions of EE (13, 14, 27, 28) and deficits in BAT thermogenesis (28–31) in mice. Collectively, these findings support a role for increased BAT thermogenesis in OT-elicited weight loss in mice. What remains unclear is whether OT-elicited weight loss requires increased sympathetic nervous system (SNS) outflow to IBAT and whether this effect involves hindbrain OT receptors (OTRs). Here, we sought to clarify the role of SNS outflow to IBAT in mediating the effects of hindbrain OTR stimulation on both weight loss and BAT thermogenesis.

We hypothesized that OT-induced stimulation of SNS outflow to IBAT contributes to its ability to stimulate non-shivering BAT thermogenesis and elicit weight loss in DIO mice. We first confirmed the success of the IBAT denervation procedure by measuring IBAT norepinephrine (NE) content at 1-week post-denervation in lean mice. We subsequently determined if these effects can be translated to DIO mice at 1, 6 and 7-weeks post-sham/denervation. To assess the role of SNS innervation of BAT in contributing to OT-elicited increases in non-shivering thermogenesis in IBAT (as surrogate measure of energy expenditure), we examined the effects of acute 4V OT (1, 5 μg) on T_{IBAT} in DIO mice following bilateral surgical SNS denervation to IBAT. We next determined if SNS innervation to IBAT contributes to OT-induced weight loss by measuring the effect of bilateral surgical or sham denervation of IBAT on the ability of chronic 4V OT (16 nmol/day over 29 days) or vehicle administration to reduce body weight and adiposity. We subsequently determined if these effects were associated with a reduction of adipocyte size and energy intake.

10.3389/fendo.2024.1440070

Methods

Animals

Adult male C57BL/6J mice were initially obtained from Jackson Laboratory [strain # 000664 (lean) or 380050 (DIO); Bar Harbor, ME] after having been maintained on a chow diet (~16 weeks; 25-35 grams upon arrival) or the high fat diet (HFD) for 4 months starting at 6 weeks of age (~22 weeks; 40-50 grams upon arrival). The chow diet provided 16% kcal from fat (~0.62% sucrose) (5LG4; LabDiet®, St. Louis, MO). The HFD provided 60% kcal from fat (~ 6.8% kcal from sucrose and 8.9% of the diet from sucrose) (Research Diets, Inc., D12492i, New Brunswick, NJ). All animals were housed individually in Plexiglas cages in a temperature-controlled room (22 ± 2°C) under a 12:12-h light-dark cycle. All mice were maintained on a 6 a.m./6 p.m. light cycle. Mice had *ad libitum* access to water and HFD. The research protocols were approved both by the Institutional Animal Care and Use Committee of the Veterans Affairs Puget Sound Health Care System (VAPSHCS) and the University of Washington in accordance with NIH Guidelines for the Care and Use of Animals.

Drug preparation

Fresh solutions of OT acetate salt were prepared the day of each experiment (Study 5). Fresh solutions of OT acetate salt (Bachem Americas, Inc., Torrance, CA) were solubilized in sterile water, loaded into Alzet® minipumps (model 2004; DURECT Corporation, Cupertino, CA) and subsequently primed in sterile 0.9% saline at 37° C for approximately 40 hours prior to minipump implantation based on manufacturer's recommended instructions (Study 6-7). The beta 3 adrenergic receptor (β3-AR) agonist, CL 316243 (Tocris/Bio-Techne Corporation, Minneapolis, MN), was solubilized in sterile water each day of each experiment (Study 4).

SNS denervation procedure

A dissecting microscope (Leica M60/M80; Leica Microsystems, Buffalo Grove, IL) was used throughout the procedure. A 1" midline incision was made in the skin dorsally at the level of the thorax and continued rostrally to the base of the skull. Connective tissue was blunt dissected away from the adipose tissue with care to avoid cutting the large thoracodorsal artery that is located medially to both pads. Both left and right fat pads were separated from the mid line. Each fat pad was lifted up and the intercostal nerve bundles were located below. Once the nerves were located, a sharp point forceps was used to pull the nerve bundles straight up while using a 45 degree scissors to cut and remove 3-5 mm of nerves. The interscapular incision was closed with 4-0 non-absorbable monofilament Ethilon (nylon) sutures or with standard metal wound clips. Nerves were similarly identified but not cut for sham operated animals. Mice were treated pre-operatively with the analgesic ketoprofen (2 mg/kg; Fort Dodge Animal Health) prior to the completion of the denervation or sham procedure. This procedure was combined with transponder implantations for studies that involved IBAT temperature measurements in response to acute 4V injections (Study 5). Animals were allowed to recover for approximately 5-7 days prior to implantation of 4V cannulas. Note that surgical denervation was used in place of chemical denervation because chemical denervation can result in SNS terminal recovery within IBAT (32, 33) within only 10 days post-chemical denervation (32).

4V cannulations for acute injections

Animals were implanted with a cannula (P1 Technologies, Roanoke, VA) that was directed towards the 4V as previously described (22). Briefly, mice under isoflurane anesthesia were placed in a stereotaxic apparatus with the incisor bar positioned 4.5 mm below the interaural line. A 26-gauge cannula (P1 Technologies) was stereotaxically positioned into the 4V (5.9 mm caudal to bregma; 0.4 mm lateral to the midline, and 2.7 mm ventral to the skull surface) and secured to the surface of the skull with dental cement and stainless-steel screws.

4V cannulations for chronic infusions

Mice were implanted with a cannula within the 4V with a side port that was connected to an osmotic minipump (model 2004, DURECT Corporation) as previously described (22). Mice under isoflurane anesthesia were placed in a stereotaxic apparatus with the incisor bar positioned 4.5 mm below the interaural line. A 30-gauge cannula (P1 Technologies) was stereotaxically positioned into the 4V (5.9 mm caudal to bregma; 0.4 mm lateral to the midline, and 3.7 mm ventral to the skull surface) and secured to the surface of the skull with dental cement and stainless steel screws. A 1.2" piece of plastic Tygon™ Microbore Tubing (0.020" x 0.060"OD; Cole-Parmer) was tunneled subcutaneously along the midline of the back and connected to the 21-gauge sidearm osmotic minipump-cannula assembly. A stainless steel 22-gauge pin plug (Instech Laboratories, Inc.) was temporarily inserted at the end of the tubing during a two week postoperative recovery period, after which it was replaced by an osmotic minipump (DURECT Corporation) containing saline or OT. Mice were treated with the analgesic ketoprofen (5 mg/kg; Fort Dodge Animal Health) and the antibiotic enrofloxacin (5 mg/kg; Bayer Healthcare LLC., Animal Health Division Shawnee Mission, KS) at the completion of the 4V cannulations and were allowed to recover at least 10 days prior to implantation of osmotic minipumps.

Implantation of temperature transponders underneath IBAT

Animals were anesthetized with isoflurane and had the dorsal surface along the upper midline of the back shaved. The area was subsequently scrubbed with 70% ethanol followed by betadine swabs to sterilize/clean the area before a one-inch incision was

made at the midline of the interscapular area. The temperature transponder (14 mm long/2 mm wide) (HTEC IPTT-300; BIO MEDIC DATA SYSTEMS, INC, Seaford, DE) was implanted underneath both IBAT pads as previously described (22) and secured in place by suturing it to the brown fat pad with sterile silk suture. HTEC IPTT-300 transponders were used in place of IPTT-300 transponders to enhance accuracy in our measurements. The IPTT-300 transponders are specified to be accurate to ± 0.4°C between 35°C and 39°C (± 1.0°C between 32°C and 42°C) while the HTEC IPTT-300 transponders are accurate to ± 0.2°C between 32°C and 42°C (personal communication with Geoff Hunt from BIO MEDIC DATA SYSTEMS). The interscapular incision was closed with Nylon sutures (5-0), which were removed in awake animals 10-14 days after surgery.

Acute 4V injections and measurements of T_{IBAT}

OT (or saline vehicle; 1 µL injection volume) was administered into the 4V immediately prior to the start of the dark cycle following 4 hours of food deprivation. Animals remained without access to food for an additional 4 h during the T_{IBAT} measurements to prevent the confounding effects of diet-induced thermogenesis on T_{IBAT}. A handheld reader (DAS-8007-IUS Reader System; BIO MEDIC DATA SYSTEMS, INC) was used to collect measurements of T_{IBAT}. The 4V injections were administered at 1 µL/min using an injection pump (Harvard Apparatus Pump II Elite; Harvard Apparatus, Holliston, MA) via a 33-gauge injector (P1 Technologies) connected by polyethylene 20 tubing to a 10-µL Hamilton syringe. Mice underwent all treatments (unless otherwise noted) in a randomized order separated by at least 48 hours between treatments.

Body composition

Determinations of lean body mass and fat mass were made on un-anesthetized mice by quantitative magnetic resonance using an EchoMRI 4-in-1-700™ instrument (Echo Medical Systems, Houston, TX) at the VAPSHCS Rodent Metabolic Phenotyping Core. Measurements were taken prior to 4V cannulations and minipump implantations as well as at the end of the infusion period.

Tissue collection for NE content measurements

Mice were euthanized by rapid conscious decapitation at 1-week (Studies 1-3), 6-weeks (Study 2), 7-weeks (Study 2, Study 6), 9-weeks (Study 4) or 10-11 weeks (Study 5) post-sham or denervation procedure. Trunk blood and tissues (IBAT, EWAT, IWAT, liver or pancreas) were collected from 4-h fasted mice. Tissue was rapidly removed, wrapped in foil and frozen in liquid N2. Samples were stored frozen at -80°C until analysis. Note that anesthesia was not used when collecting tissue for NE content as it can cause the release of NE from SNS terminals within the tissue (33). Thus, animals were euthanized by rapid conscious decapitation.

Norepinephrine content measurements (biochemical confirmation of IBAT denervation procedure)

NE content was measured in IBAT, EWAT, IWAT, liver and/or pancreas using previously established techniques (34). Successful denervation was noted by ≥ 60% reduction in IBAT NE content as previously noted (35). Experimental animals that did not meet this criterion were excluded from the data analysis.

Study protocols

Study 1A: determine the success of the surgical denervation procedure at 1-week post-sham or denervation in lean mice by measuring NE content

Mice underwent sham or bilateral surgical SNS denervation procedures and, to prevent the confounder of anesthesia on NE content, animals were euthanized by rapid conscious decapitation at 1-week post-sham or denervation procedure.

Study 1B: determine the success of the surgical denervation procedure at 10-12 weeks post-sham or denervation in lean mice by measuring thermogenic gene expression

Mice underwent sham or bilateral surgical SNS denervation procedures and were euthanized by rapid conscious decapitation at 1-week post-sham or denervation procedure.

Study 2: determine the success of the surgical denervation procedure at 1-, 6- and 7-weeks post-sham or denervation in DIO mice by measuring NE content

Mice were fed *ad libitum* and maintained on HFD for approximately 4.25 months prior to underdoing sham or SNS denervation procedures. In addition to weekly body weight measurements, body composition measurements were obtained at baseline and at 6 and 7-weeks post-denervation/sham procedures. Mice were euthanized by rapid conscious decapitation 1-, 6- and 7-weeks post-sham or denervation procedure.

Study 3: determine if SNS innervation of IBAT is reduced in age-matched obese mice relative to lean mice by measuring NE content

Chow-fed and HFD-fed mice were age-matched (~22 weeks; 30-35 grams or 40-50 grams upon arrival). Age-matched chow-fed and DIO mice were fed *ad libitum* and maintained on chow or HFD for 4.5 months and matched for both body weight and adiposity prior to undergoing sham (N=5/diet) or SNS denervation (N=5/diet) procedures. Mice were euthanized by rapid conscious decapitation at 1-week post-sham or denervation procedure.

Study 4: determine if surgical denervation of IBAT compromises the ability of the β3-AR agonist, CL 316243, to increase T_{IBAT} in DIO mice

Mice were fed *ad libitum* and maintained on HFD for 4.5 months prior to underdoing sham or SNS denervation procedures and implantation of temperature transponders underneath the left IBAT depot. Mice were allowed to recover for at least 1 week during which time they were adapted to a daily 4-h fast, handling and mock injections. On an experimental day, 4-h fasted mice received CL 316243 (0.1 or 1 mg/kg; IP) or vehicle (sterile water; 1.5 mL/kg injection volume) during the early part of the light cycle in order to maximize the effects of CL 316243 during a time when circulating NE levels (36) and IBAT catecholamine levels are lower (37). Injections were completed in a crossover design at 7-day intervals such that each animal served as its own control (approximately 4-6 weeks post-sham or denervation procedures). T_{IBAT} was measured at baseline (-2 h; 8:00 a.m.), immediately prior to IP injections (0 h; 9:45-10:00 a.m.), and at 0.25, 0.5, 0.75, 1, 1.25, 1.5, 2, 3, 4, and 24-h post-injection (9:45-10:00 a.m.). Food intake and body weight were measured daily. This dose range was based on doses of CL 316243 found to be effective at reducing food intake and weight gain in rats (22, 38) (IP) and stimulating IBAT temperature in rats (22, 39) (IV, IP) and mice (IV) (40). Animals were euthanized by rapid conscious decapitation at 9-weeks post-sham or denervation procedure. Similar studies were also performed in lean mice (data not shown).

Likewise, we also examined the effects of systemic administration of the transient receptor potential channel melastatin family member 8 (TRPM8) agonist, icilin, which, may activate IBAT through a direct (41) or indirect mechanism (42) (data not shown). In addition, the effects of the sympathomimetic, tyramine, was also examined on T_{IBAT} in DIO mice with intact or impaired SNS innervation of IBAT (Supplementary Study 1).

Study 5: determine the extent to which 4V OT-induced activation of sympathetic outflow to IBAT contributes to its ability to increase T_{IBAT} in DIO mice

Mice were fed *ad libitum* and maintained on HFD for 4.25 months prior to undergoing sham or SNS denervation procedures and implantation of temperature transponders underneath the left IBAT depot. Mice were subsequently implanted 1 week later with 4V cannulas. Mice were allowed to recover for at least 2 weeks during which time they were adapted to a daily 4-h fast, handling and mock injections. On an experimental day, 4-h fasted mice received OT (1 or 5 μg/μl) or vehicle during the early part of the light cycle in order to maximize the effects of OT (14, 22) during a time when circulating NE levels (36) and IBAT catecholamine levels are lower (37). Injections were completed in a crossover design at approximately 48-h intervals such that each animal served as its own control (approximately 7-8 weeks post-sham or denervation procedures). T_{IBAT} was measured at baseline (-2 h; 9:00 a.m.), immediately prior to 4V injections (0 h; 9:45-10:00 a.m.), and at 0.25, 0.5, 0.75, 1, 1.25, 1.5, 2, 3, 4, and 24-h post-injection (10:00 a.m.). Food intake and body weight were measured daily. This dose range was based on doses of 4V OT found to be effective at stimulating T_{IBAT} in DIO mice in previous studies (22). Mice were euthanized by rapid conscious decapitation at 10-11 weeks post-sham or denervation procedure.

Similar studies were also performed in lean mice (Supplementary Study 2). In addition, we examined the effectiveness of a systemic dose to recapitulate the effects of a 4V dose to increase T_{IBAT} in lean mice (Supplementary Study 3). We next determined if the melanocortin 3/4 receptor (MC3/4R) agonist, melanotan II (MTII), which, along with the endogenous MC3/4R agonist, alpha-MSH, activate PVN OT neurons (43, 44) and act, in part, through OT signaling (43, 45), could recapitulate the effects of systemic OT on T_{IBAT} in lean mice with intact or impaired SNS innervation of IBAT (data not shown).

Study 6A: determine the extent to which OT-induced activation of sympathetic outflow to IBAT contributes to its ability to elicit weight loss in DIO mice

Mice were fed *ad libitum* and maintained on HFD for 4.25-4.5 months prior to prior to undergoing sham or SNS denervation procedures and implantation of temperature transponders underneath the left IBAT depot. Mice subsequently received 4V cannulas and minipumps to infuse vehicle or OT (16 nmol/day) over 28 days as previously described (22). This dose was selected based on a dose of 4V OT found to be effective at reducing body weight in DIO mice (22). Daily food intake and body weight were also tracked for 28 days. Animals were euthanized by rapid conscious decapitation at 7 weeks post-sham or denervation procedure.

Study 6B: determine the extent to which OT-induced activation of sympathetic outflow to IBAT impacts thermogenic gene expression in IBAT, IWAT, and EWAT in DIO mice

Mice from Study 6A were used for these studies. All mice were euthanized by rapid conscious decapitation following a 4-h fast at 2-h post-injection.

Study 7: determine the extent to which systemic (subcutaneous) infusion of a centrally effective dose of OT (16 nmol/day) elicits weight loss in DIO mice

Mice were fed *ad libitum* and maintained on HFD for 4-4.25 months prior to prior to being implanted with a temperature transponder underneath the left IBAT depot. Mice were subsequently maintained on a daily 4-h fast and received minipumps to infuse vehicle or OT (16 nmol/day) over 28 days (22). This dose was selected based on a dose of 4V OT found to be effective at reducing body weight in DIO mice (22). Daily food intake and body weight were also tracked for 28 days. Mice were euthanized with intraperitoneal injections of ketamine cocktail [ketamine hydrochloride (390 mg/kg), xylazine (26.4mg/kg) in an injection volume up to 1 mL/mouse] prior to collection of blood (cardiac stick) and tissues (IBAT, EWAT, IWAT, gastrocnemius and brain). Tissue was otherwise treated identically to Studies 1-4 or processed for subsequent measurements of adipocyte size and UCP-1 (see below).

Blood collection

Blood samples [trunk blood (Study 3-6) or cardiac stick (Study 7)] were collected from 4-h (Study 2-7) or 6-h (Study 1B) fasted mice within a 2-h window towards the beginning of the light cycle (10:00 a.m.-12:00 p.m.) as previously described in DIO CD ® IGS and Long-Evans rats and C57BL/6J mice (21, 22, 46). Treatment groups were counterbalanced at time of euthanasia to avoid time of day bias. Blood samples [up to 1 mL] were collected by trunk blood or cardiac stick in chilled K2 EDTA Microtainer Tubes (Becton-Dickinson, Franklin Lakes, NJ). Whole blood was centrifuged at 6,000 rpm for 1.5-min at 4°C; plasma was removed, aliquoted and stored at −80°C for subsequent analysis.

Plasma hormone measurements

Plasma leptin and insulin were measured using electrochemiluminescence detection [Meso Scale Discovery (MSD®), Rockville, MD] using established procedures (21, 47). Intra-assay coefficient of variation (CV) for leptin was 4.2% and 1.9% for insulin. The range of detectability for the leptin assay is 0.137-100 ng/mL and 0.069-50 ng/mL for insulin. Plasma fibroblast growth factor-21 (FGF-21) (R&D Systems, Minneapolis, MN) and irisin (AdipoGen, San Diego, CA) levels were determined by ELISA. The intra-assay CV for FGF-21 and irisin were 2.3% and 9.3%, respectively; the ranges of detectability were 31.3-2000 pg/mL (FGF-21) and 0.078-5 µg/mL (irisin). Plasma adiponectin was determined by ELISA [Millipore Sigma (Burlington, MA)]. Intra-assay CV for adiponectin was 4.2%. The range of detectability for the adiponectin assay is 2.8-178 ng/mL. The data were normalized to historical values using a pooled plasma quality control sample that was assayed in each plate.

Blood glucose and lipid measurements

Blood was collected for glucose measurements by tail vein nick in 4-h fasted mice and measured with a glucometer using the AlphaTRAK 2 blood glucose monitoring system (Abbott Laboratories, Abbott Park, IL) (21, 48). Total cholesterol (TC) [Fisher Diagnostics (Middletown, VA)], free fatty acids (FFAs) [Wako Chemicals USA, Inc., Richmond, VA)] and free glycerol (FG) (Millipore Sigma) were measured using an enzymatic-based kits. Intra-assay CVs for TC, FFAs and FG were 1.5, 2.9, and 2.2%, respectively. These assay procedures have been validated for rodents (49).

Adipose tissue processing for adipocyte size

Adipose tissue depots were collected at the end of the infusion period from a subset of DIO mice from Study 6 (IBAT, IWAT, EWAT) and Study 7 (EWAT and IWAT). IBAT, IWAT, and EWAT depots were dissected and placed in 4% paraformaldehyde-PBS for 24 h and then placed in 70% ethanol (EtOH) prior to paraffin embedding. Sections (5 µm) sampled were obtained using a rotary microtome, slide-mounted using a floatation water bath (37°C), and baked for 30 min at 60°C to give approximately 15-16 slides/fat depot with two sections/slide.

Adipocyte size analysis

Adipocyte size analysis was performed on deparaffinized and digitized IWAT and EWAT sections. The average cell area from two randomized photomicrographs was determined using the built-in particle counting method of ImageJ software (National Institutes of Health, Bethesda, MD). Fixed (4% PFA), paraffin-embedded adipose tissue was sectioned. Slides were visualized using bright field on an Olympus BX51 microscope (Olympus Corporation of the Americas; Center Valley, PA) and photographed using a Canon EOS 5D SR DSLR (Canon U.S.A., Inc., Melville, NY) camera at 100X magnification. Values for each tissue within a treatment were averaged to obtain the mean of the treatment group.

Tissue collection for NE content measurements

Mice were euthanized by rapid conscious decapitation at 1-week (Studies 1-3), 6-weeks (Study 2), 7-weeks (Study 2, Study 6), 9-weeks (Study 4) or 10-11 weeks (Study 5) post-sham or denervation procedure. Trunk blood and tissues (IBAT, EWAT, IWAT, liver or pancreas) were collected from 4-h (Study 2-7) or 6-h (Study 1B) fasted mice. Tissue was rapidly removed, wrapped in foil and frozen in liquid N2. Samples were stored frozen at -80°C until analysis. Note that anesthesia was not used when collecting tissue for NE content as it can cause the release of NE from SNS terminals within the tissue (33).

Tissue collection for quantitative real-time PCR

Tissue (IBAT, IWAT and EWAT) was collected from a subset of 4-h (Study 2-7) or 6-h (Study 1B) fasted mice in Study 4-7. In addition, mice from Study 7 were euthanized with an overdose of ketamine cocktail prior to tissue collection. IBAT, IWAT, EWAT, gastrocnemius and brains were collected within a 2-h window towards the start of the light cycle (10:00 a.m.-12:00 p.m.) as previously described in DIO CD ® IGS/Long-Evans rats and C57BL/6J mice (21, 22, 46). Tissue was rapidly removed, wrapped in foil and frozen in liquid N2. Samples were stored frozen at -80°C until analysis.

qPCR

RNA extracted from samples of IBAT and IWAT (Studies 4-7) were analyzed using the RNeasy Lipid Mini Kit (Qiagen Sciences Inc, Germantown, MD) followed by reverse transcription into

cDNA using a high-capacity cDNA archive kit (Applied Biosystems, Foster City, CA). Quantitative analysis for relative levels of mRNA in the RNA extracts was measured in duplicate by qPCR on an Applied Biosystems 7500 Real-Time PCR system (Thermo Fisher Scientific, Waltham, MA) and normalized to the cycle threshold value of Nono mRNA in each sample. The TaqMan® probes used in the study were Thermo Fisher Scientific Gene Expression Assay probes. The probe for mouse Nono (Mm00834875_g1), UCP-1 (catalog no. Mm01244861_m1), UCP-2 (catalog no. Mm00627599_m1), UCP-3 (catalog no. Mm01163394_m1), β1-AR (Adrb1; catalog no. Mm00431701_s1), β2-AR (Adrb2; catalog no. Mm02524224_s1), β3-AR (Adrb3; catalog no. Mm02601819_g1), alpha-2 adrenergic receptor (Adra2a; catalog no. Mm07295458_s1),type 2 deiodinase (D2) (Dio2; catalog no. Mm00515664_m1), cytochrome c oxidase subunit 8b (Cox8b; catalog no. Mm00432648_m1), G-protein coupled receptor 120 (Gpr120; catalog no. Mm00725193_m1), bone morphogenetic protein 8b (bmp8b; catalog no. Mm00432115_g1), cell death-inducing DNA fragmentation factor alpha-like effector A (Cidea; catalog no. Mm00432554_m1), peroxisome proliferator-activated receptor gamma coactivator 1 alpha (Ppargc1a; catalog no. Mm01208835_m1) were acquired from Thermo Fisher Scientific. Relative amounts of target mRNA were determined using the Comparative C_T or $2^{-\Delta\Delta CT}$ method (50) following adjustment for the housekeeping gene, Nono.

Transponder placement

All temperature transponders were confirmed to have remained underneath the IBAT depot at the conclusion of the study.

Statistical analyses

All results are expressed as means ± SE. Comparisons between multiple groups involving between subjects design were made using one-way ANOVA as appropriate, followed by a *post-hoc* Fisher's least significant difference test. Comparisons involving within-subjects designs were made using a one-way repeated-measures ANOVA followed by a *post-hoc* Fisher's least significant difference test. Analyses were performed using the statistical program SYSTAT (Systat Software, Point Richmond, CA). Differences were considered significant at $P<0.05$, 2-tailed.

Results

Study 1A: determine the success of the surgical denervation procedure at 1-week post-sham or denervation in lean mice

The goal of this study was to verify the success of the SNS denervation of IBAT procedure in lean mice by confirming a reduction of NE content that was specific to IBAT relative to other tissues (IWAT and liver). By design, mice were lean as determined by body weight (25.4 ± 0.3 g). There was no difference in body weight between sham and denervation groups prior to surgery (sham: 25.8 ± 0.3 g vs denervation: 25.1 ± 0.5 g) [($F(1,8) = 1.923$, $P=0.203$)] or at 1-week post-surgery (sham: 26.3 ± 0.4 g vs denervation: 26.1 ± 0.7 g) [($F(1,8) = 0.021$, $P=0.888$)].

IBAT NE content was reduced by 99.6 ± 0.2% at 1-week post-denervation [($F(1,8) = 12.358$, $P=0.008$)] (Figure 1) relative to IBAT from sham operated mice. In contrast, NE content was unchanged in IWAT or liver in denervated mice relative to sham mice (P=NS). We also repeated this study in a separate group of lean mice and found a similar reduction of IBAT NE content (99.2 ± 0.4%) at 1-week post-denervation relative to sham operated mice [($F(1,8) = 73.438$, $P=0.000$)].

Study 1B: verify the success of the surgical denervation procedure at 10-12 weeks after IBAT surgical denervation or sham denervation in lean mice by measuring thermogenic gene expression

The goal of this study was to determine the 1) verify the success of the SNS denervation of IBAT procedure in lean mice using a separate biochemical marker (IBAT thermogenic gene expression) and 2) confirm that these changes would persist for extended periods of time out to 10-12 weeks. There was no difference in body weight between sham and denervation groups prior to surgery (sham: 43.8 ± 1.3 g vs denervation: 43.0 ± 0.98 g) [($F(1,17) = 0.238$, $P=0.632$)] or at 10-12 weeks post-surgery (sham: 50.5 ± 2.0 g vs denervation: 49.3 ± 1.1 g) [($F(1,17) = 0.292$, $P=0.596$)].

IBAT NE content was reduced in denervated mice by 96.1 ± 3.3% at 10-12 weeks after IBAT surgical denervation relative to sham-operated control mice [($F(1,2) = 87.393$, $P=0.011$). Only a subset of samples (N=4 out of 20) were able to be screened for NE content but all tissue samples were included in the IBAT (N=20 out of 20), IWAT (N=9 out of 20) and EWAT (N=9 out of 20) gene expression analysis.

IBAT

There was a reduction of 9 out of the 13 measured mRNA levels of genes from IBAT of denervated mice relative to IBAT from sham operated mice ($P<0.05$; Table 1A).There were significant reductions of IBAT UCP-1 [($F(1,7) = 38.1$, $P<0.001$)], Dio2 [($F(1,7) = 12.669$, $P=0.009$)], Gpr120 [($F(1,7) = 65.965$, $P<0.001$)], Adrb3 [($F(1,7) = 65.916$, $P<0.001$)], Adrb1 [($F(1,7) = 8.015$, $P=0.025$)], Acox1 [($F(1,7) = 58.261$, $P<0.001$)], bmp8b [($F(1,7) = 19.636$, $P=0.003$)], cox8b [($F(1,6) = 16.403$, $P=0.007$)] and UCP-3 mRNA expression [($F(1,7) = 57.665$, $P<0.001$)]. There were no significant differences in IBAT CIDEA, PPARGC1, PPARA and PRDM16 mRNA expression between sham and denervation groups (P=NS).

The findings pertaining to IBAT UCP-1 gene expression in surgically denervated mice is consistent with what others have reported with IBAT UCP-1 protein expression from hamsters

10.3389/fendo.2024.1440070

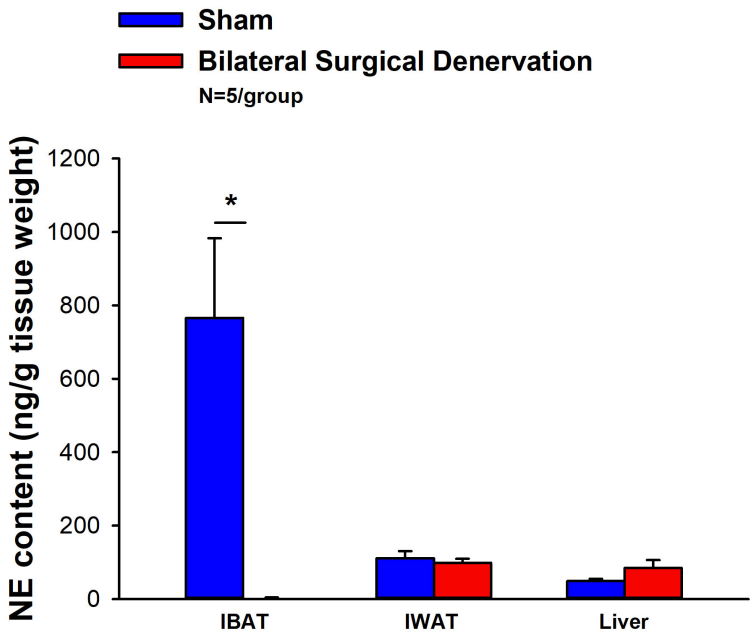

FIGURE 1
Effect of IBAT surgical denervation procedure on IBAT NE content at 1-week post-sham or IBAT denervation in lean mice. Mice were maintained on chow for approximately 2.5 months prior to undergoing a sham (N=5/group) or bilateral surgical IBAT denervation (N=5/group) procedures and were euthanized at 1-week post-sham or denervation procedure. NE content was measured from IBAT, IWAT and liver. Data are expressed as mean ± SEM. *P<0.05 denervation vs sham.

(51) and mice (52) following chemical (6-OHDA)-induced denervation of IBAT relative to control animals. Similarly, there was a reduction of IBAT UCP-1 mRNA following unilateral or bilateral surgical denervation in hamsters (53) and mice (54, 55), respectively. Similar to our findings, others also found a reduction of IBAT Dio2 and Adrb3 following bilateral surgical denervation in mice (54).

IWAT

IWAT UCP-1 [(F(1,2) = 11.131, P=0.079)] tended to be elevated in denervated mice relative to sham operated mice (Table 1B). There were no significant differences in the mRNAs of any of the other thermogenic markers (P=NS; Table 1B).

EWAT

There tended to be a reduction of UCP-1 in denervated mice compared to sham operated mice [(F(1,2) = 7.000, P=0.118)] (Table 1C). There were no significant differences in the mRNA levels of any of the other thermogenic genes (P=NS; Table 1C).

Study 2: determine the success of the surgical denervation procedure at 1, 6 and 7-weeks post-sham or denervation in DIO mice

The goal of this study was to 1) verify the success of the SNS denervation procedure in DIO mice by confirming a reduction of NE content that was specific to IBAT relative to other tissues (IWAT, liver and pancreas) and 2) confirm that these changes would persist for 7 weeks. By design, DIO mice were obese as determined by both body weight (45.1 ± 1.1 g) and adiposity (14.9 ± 0.8 g fat mass; 32.9 ± 1.3% adiposity) after maintenance on the HFD for approximately 4.5 months prior to sham/denervation procedures. Sham and denervation groups were matched for body weight, fat mass and lean mass such that there were no differences in baseline body weight, lean mass or fat mass between groups prior to surgery (data not shown; P=NS).

IBAT NE content was reduced by 95.9 ± 2.0, 77.4 ± 12.7 and 93.6 ± 4.6% at 1- [(F(1,8) = 19.636, P=0.002)], 6- [(F(1,8) = 20.532, P=0.002)] and 7-weeks [(F(1,8) = 34.586, P<0.0001)] post-denervation (Figure 2) relative to IBAT from sham operated mice. In contrast, NE content was unchanged in IWAT, liver or pancreas in denervated mice relative to sham mice (P=NS).

There were no significant differences in baseline body weights [(F(5,24) = 0.322, P=NS), fat mass [(F(5,24) = 0.106, P=NS), or lean mass [(F(5,24) = 0.304, P=NS) between sham and denervation groups. In addition, there were also no significant differences in body weights between sham and denervation groups at 1- [(F(1,8) = 0.353, P=NS), 6- [(F(1,8) = 1.230, P=NS) and 7-weeks [(F(1,8) = 0.109, P=NS) post-surgeries. In addition, there were also no significant differences in fat mass at 1- [(F(1,8) = 0.353, P=NS), 6- [(F(1,8) = 1.230, P=NS) and 7-weeks [(F(1,8) = 0.109, P=NS) post-denervation relative to sham operated mice. Similarly, no differences were found in lean mass at 1- [(F(1,8) = 0.141, P=NS)], 6- [(F(1,8) = 0.015, P=NS)] and 7-weeks [(F(1,8) = 0.009, P=NS)] post-

10.3389/fendo.2024.1440070

TABLE 1A Changes in IBAT mRNA expression following IBAT denervation.

Treatment	SHAM	DENERVATION
IBAT	4V VEH	4V VEH
Adrb1	1.0 ± 0.1[a]	0.6 ± 0.1[b]
Adrb3	1.0 ± 0.1[a]	0.3 ± 0.03[b]
Acox1	1.0 ± 0.1[a]	0.4 ± 0.03[b]
UCP1	1.0 ± 0.1[a]	0.3 ± 0.1[b]
UCP3	1.0 ± 0.04[a]	0.4 ± 0.1[b]
bmp8b	1.0 ± 0.2[a]	0.2 ± 0.1[b]
Cidea	1.0 ± 0.1[a]	0.9 ± 0.1[a]
Gpr120	1.0 ± 0.1[a]	0.1 ± 0.03[b]
Cox8b	1.0 ± 0.1[a]	0.7 ± 0.1[b]
DIO2	1.0 ± 0.2[a]	0.3± 0.1[b]
PRDM16	1.0 ± 0.2[a]	0.8 ± 0.1[a]
Ppargc1a	1.0 ± 0.1[a]	0.7 ± 0.1[a]
Ppara	1.0 ± 0.1[a]	0.8 ± 0.1[a]

IBAT was collected at 2-h post-injection of 4V Vehicle (VEH).
Different letters denote significant differences between treatments.
Shared letters are not significantly different from one another.
Data are expressed as mean ± SEM.
N=3-6/group.

TABLE 1B Changes in IWAT mRNA expression following IBAT denervation.

Treatment	SHAM	DENERVATION
IBAT	4V VEH	4V VEH
Adrb1	1.0 ± 0.1[a]	0.7 ± 0.1[a]
Adrb3	1.0 ± 0.5[a]	0.9 ± 0.2[a]
Acox1	1.0 ± 0.6[a]	1.0 ± 0.6[a]
UCP1	1.0 ± 0.2[a]	13.6 ± 3.8[a]
UCP3	1.0 ± 0.4[a]	1.1 ± 0.03[a]
bmp8b	1.0 ± 0.5[a]	1.3 ± 0.6[a]
Cidea	1.0 ± 0.4[a]	1.5 ± 0.3[a]
Gpr120	1.0 ± 0.2[a]	0.9 ± 0.1[a]
Cox8b	1.0 ± 0.1[a]	2.5 ± 1.6[a]
DIO2	1.0 ± 0.01[a]	4.0 ± 2.4[a]
Ppargc1a	1.0 ± 0.7[a]	0.9 ± 1.1[a]
Ppara	1.0 ± 0.7[a]	0.8 ± 0.8[a]

IWAT was collected at 2-h post-injection of 4V Vehicle (VEH).
Different letters denote significant differences between treatments.
Shared letters are not significantly different from one another.
Data are expressed as mean ± SEM.
N=2/group.

TABLE 1C Changes in EWAT mRNA expression following IBAT denervation.

Treatment	SHAM	DENERVATION
IBAT	4V VEH	4V VEH
Adrb1	1.0 ± 0.4[a]	1.0 ± 0.2[a]
Adrb3	1.0 ± 0.4[a]	1.1 ± 0.1[a]
Acox1	1.0 ± 0.2[a]	1.1 ± 0.01[a]
UCP1	1.0 ± 0.04[a]	0.7 ± 0.1[a]
UCP3	1.0 ± 0.4[a]	0.9 ± 0.01[a]
bmp8b	1.0 ± 0.2[a]	0.9 ± 0.1[a]
Cidea	1.0 ± 0.6[a]	1.5 ± 0.4[a]
Gpr120	1.0 ± 0.1[a]	1.0 ± 0.1[a]
Cox8b	1.0 ± 0.3[a]	1.9 ± 0.6[a]
DIO2	1.0 ± 0.2[a]	1.7 ± 0.4[a]
Ppargc1a	1.0 ± 0.4[a]	1.3 ± 0.03[a]

EWAT was collected at 2-h post-injection of 4V Vehicle (VEH).
Different letters denote significant differences between treatments.
Shared letters are not significantly different from one another.
Data are expressed as mean ± SEM.
N=2/group.

denervation relative to sham operated mice. These findings are in agreement with others who have reported no difference in body weight (51, 52, 54–56) or fat mass (52, 55) in hamsters or mice following bilateral surgical or chemical denervation of IBAT.

Study 3: determine if SNS innervation of IBAT is reduced in age-matched obese mice relative to lean mice

The goal of this study was to determine if SNS innervation to IBAT is reduced in the obese state relative to lean animals. Given that SNS activation of BAT and BAT activity decline with age [(57); for review see (58)], DIO mice were age-matched to lean chow-fed control mice. By design, DIO mice were obese as determined by both body weight (46.4 ± 1.2 g) and adiposity (17.8 ± 0.7 g fat mass; 38.3 ± 0.8% adiposity) relative to age-matched chow-fed control mice (33.1 ± 0.4 g) and adiposity (6.3 ± 0.4 g fat mass; 18.9 ± 1.1% adiposity) after maintenance on the HFD and chow, respectively, for approximately 4.5 months prior to sham procedures.

IBAT NE content was reduced by 38.9 ± 9.8% relative in lean mice relative to age-matched DIO mice [($F(1,8) = 10.757$, $P=0.011$)] (Figure 3). In addition, NE content in IWAT [($F(1,8) = 19.363$, $P=0.002$)] and liver [($F(1,8) = 14.516$, $P=0.005$)] was reduced in lean mice compared to age-matched DIO mice. NE content in pancreas also appeared to be reduced in lean mice relative to DIO mice [($F(1,8) = 4.233$, $P=0.074$)] while there was no significant difference in NE from EWAT (P=NS).

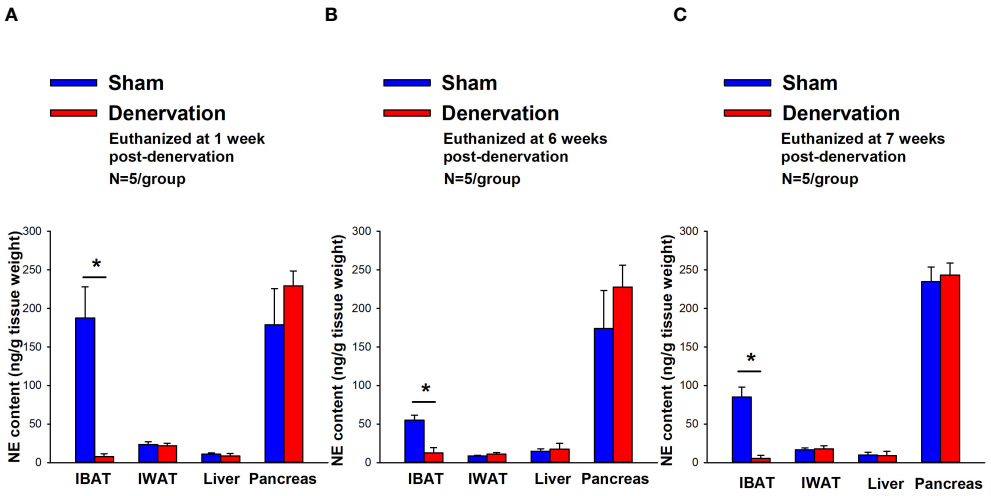

FIGURE 2
Effect of IBAT surgical denervation procedure on IBAT NE content at 1-, 6- and 7-weeks post-sham or IBAT denervation in DIO mice. Mice were maintained on a HFD (60% kcal from fat) for approximately 4.25 months prior to undergoing sham (N=5/group) or bilateral surgical IBAT denervation (N=5/group) procedures and were euthanized at **(A)** 1-, **(B)** 6- and **(C)** 7-weeks post-sham (N=15/group) or denervation procedures (N=15/group). NE content was measured from IBAT, IWAT, liver and pancreas. Data are expressed as mean ± SEM. *P<0.05, †0.05<P<0.1 denervation vs sham.

Study 4: determine if surgical denervation of IBAT changes the ability of the β3-AR agonist, CL 316243, to increase T_{IBAT} in DIO mice

The goal of this study was to verity that there was no change in the ability of IBAT to respond to direct β3-AR stimulation as a result of the denervation procedure relative to sham operated animals. By design, DIO mice were obese as determined by both body weight (44.2 ± 0.6 g) and adiposity (13.9 ± 0.8 g fat mass; 31.2 ± 1.4% adiposity) after maintenance on the HFD for approximately 4.5 months prior to sham/denervation procedures. The mice used in this study were identical to those used in Study 1B.

In sham mice, CL 316243 (1 mg/kg) increased T_{IBAT} at 0.25, 0.75, 1, 2, 3 and 4-h post-injection. The lowest dose (0.1 mg/kg) also stimulated T_{IBAT} at 0.25, 0.75, 1, 2, 3 and 4-h post-injection (P<0.05; Figure 4A). In addition, similar findings were apparent when measuring change in T_{IBAT} relative to baseline T_{IBAT} (Figure 4B). CL 316243 also stimulated T_{IBAT} and T_{IBAT} relative to baseline at 24-h post-injection at the high dose (P<0.05; data not shown).

IBAT NE content was reduced in denervated mice by 97.8 ± 0.5% in denervated mice relative to sham-operated control mice [(F(1,17) = 73.270, P<0.001). In contrast, there was no difference in NE content in IWAT, EWAT, liver or pancreas between sham or denervation groups (P=NS).

In denervated mice, CL 316243 (1 mg/kg) increased T_{IBAT} at 0.25, 0.5, 0.75, 1, 1.25, 1.5, 1.75, 2, 3 and 4-h post-injection. The lowest dose (0.1 mg/kg) also stimulated T_{IBAT} at 0.25, 0.5, 0.75, 1, 2, 3 and 4-h post-injection ((P<0.05; Figure 4C). CL 316243 also stimulated T_{IBAT} at 24-h post-injection at the high dose (P<0.05; data not shown). Similar findings were apparent when measuring change in T_{IBAT} relative to baseline T_{IBAT} through 240-min post-injection (Figure 4D). CL 316243 (1 mg/kg) also tended to stimulate the change in T_{IBAT} relative to baseline T_{IBAT} at 24-h post-injection (P=0.050).

Importantly, there was no difference in the T_{IBAT} response to CL 316243 (0.1 or 1 mg/kg) when the data were averaged over the 1-h or 4-h post-injection period between sham and denervated mice (P=NS).

Overall, these findings indicate that IBAT denervation did not change the ability of CL 316243 to increase BAT thermogenesis (surrogate measure of EE) in DIO mice relative to sham operated mice.

Energy intake

In sham mice, CL 316243 reduced daily energy intake at both 0.1 and 1 mg/kg by 25.3 and 51% (P<0.05). Similarly, in denervated mice, CL 316243 also reduced daily energy intake at both 0.1 and 1 mg/kg (P<0.05) by 34 and 57.1% relative to vehicle (Figure 4E).

Body weight

CL 316243 did not reduce overall body weight in either group. However, the high dose reduced body weight gain in both sham and denervated mice (P<0.05; Figure 4F) while the low dose also reduced body weight gain in the denervated mice (P<0.05; Figure 4F).

Importantly, there was no difference in the effectiveness of CL 316243 (0.1 or 1 mg/kg) to reduce energy intake or weight gain between sham and denervated mice (P=NS). However, there appeared to be a more enhanced effect of CL 316243 (0.1 mg/kg) to reduce weight gain (P=0.091) in the denervated group relative to the sham group.

Furthermore, there was no difference in energy intake [sham: 14.7 ± 0.98 kcal; denervation: 14.8 ± 0.8 kcal] or change in body weight [sham: -0.1± 0.2g; denervation: -0.1 ± 0.2 g] following acute IP vehicle injections in sham or denervated mice (P=NS).

Overall, these findings indicate that IBAT denervation did not change the ability of CL 316243 to reduce food intake or body weight gain in DIO mice relative to sham operated mice.

Similar results were also found in lean mice (data not shown). The sympathomimetic, icilin, which may act indirectly to stimulate BAT thermogenesis through SNS outflow to IBAT, increased T_{IBAT}

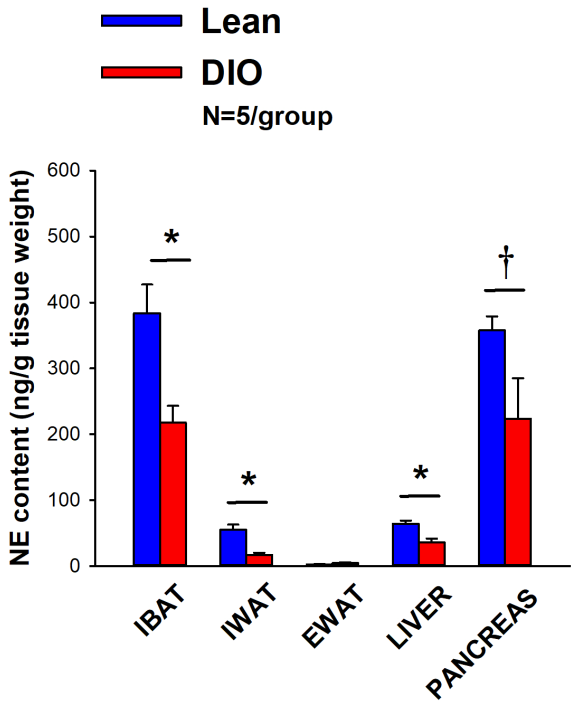

FIGURE 3
Effect of diet-induced obesity (DIO) on SNS Innervation (NE content) of IBAT, IWAT, EWAT, liver and pancreas at 1-week post-sham in age-matched lean and DIO mice. Age-matched mice were maintained on either chow (16% kcal from fat) or HFD (60% kcal from fat) for approximately 4.5 months prior to undergoing a sham denervation (N=5/group) procedure and were euthanized at 1-week post-sham (N=5/group). NE content was measured from IBAT, IWAT, EWAT, liver and pancreas. Data are expressed as mean ± SEM. *P<0.05, †0.05<P<0.1 lean vs DIO.

(P<0.05) throughout the measurement period in both sham and IBAT denervated mice (P<0.05; data not shown).

The effects of the sympathomimetic, tyramine (Supplementary Study 1), was also examined on T_{IBAT} in DIO mice with intact or impaired SNS innervation of IBAT. Tyramine (19.2 mg/kg) increased T_{IBAT} during the initial part of the measurement period in both sham and IBAT denervated mice (P<0.05; Supplementary Figures 1A–D).

There was no difference in the T_{IBAT} response to tyramine (19.2 mg/kg) when the data were averaged over the 0.25-h post-injection period between sham and denervated mice (P=NS). Similar findings were also observed when comparing T_{IBAT} or change from baseline T_{IBAT} at 0.25-h and 0.5-h post-injection between sham and denervated mice (P=NS).

Overall, these findings demonstrate there is not a functional change in the ability of IBAT to respond to direct β3-AR stimulation or other agents, including icilin, that may activate BAT through a direct non-β3-AR mechanism in denervated mice relative to sham animals.

Study 5: determine the extent to which OT-induced activation of sympathetic outflow to IBAT contributes to its ability to increase T_{IBAT} in DIO mice

After having confirmed there was no functional defect in the ability of IBAT to respond to direct β3-AR stimulation (Study 4), the goal of this study was to determine if OT-elicited elevation of T_{IBAT} requires intact SNS outflow to IBAT. By design, DIO mice were obese as determined by both body weight (43.6 ± 0.7 g) and adiposity (13.8 ± 0.6 g fat mass; 31.5 ± 1.1% adiposity) after maintenance on the HFD for approximately 4.25 months prior to sham/denervation procedures. There was no difference in body weight between sham and denervation groups prior to surgery (sham: 43.0 ± 1.1 g vs denervation: 42.9 ± 1.1 g) [($F(1,19) = 0.005$, P=0.943] or at 10-11 weeks post-surgery (sham: 44.8 ± 1.8 g vs denervation: 43.9 ± 2.8 g) [($F(1,19) = 0.069$, P=0.796]. Note that the T_{IBAT} data from sham-operated DIO mice has been previously published (22).

IBAT NE content was reduced by 94.9 ± 3.3% in denervated mice relative to sham-operated control mice [($F(1,19) = 33.427$, P<0.001). In contrast, there was no difference in NE content in IWAT, EWAT, liver or pancreas between sham or denervation groups (P=NS).

In sham mice, 4V OT (5 µg) increased T_{IBAT} at 1 and 1.25-h post-injection (P<0.05) and tended to stimulate T_{IBAT} at 0.75, 1.5 and 1.75-h post-injection (0.05<P<0.1). The lowest dose (1 µg) also stimulated T_{IBAT} at 0.75 and 1-h post-injection and tended to stimulate T_{IBAT} at 1.25-h post-injection (0.05<P<0.1; Figure 5A). Similar findings were apparent when measuring change in T_{IBAT} relative to baseline T_{IBAT} (Figure 5B).

In denervated mice, OT (5 µg) increased T_{IBAT} at 0.75, 1, 1.25, 1.5, 2 and 3-h post-injection (P<0.05). The lowest dose (1 µg) tended to stimulate T_{IBAT} at 4-h and 24-h post-injection

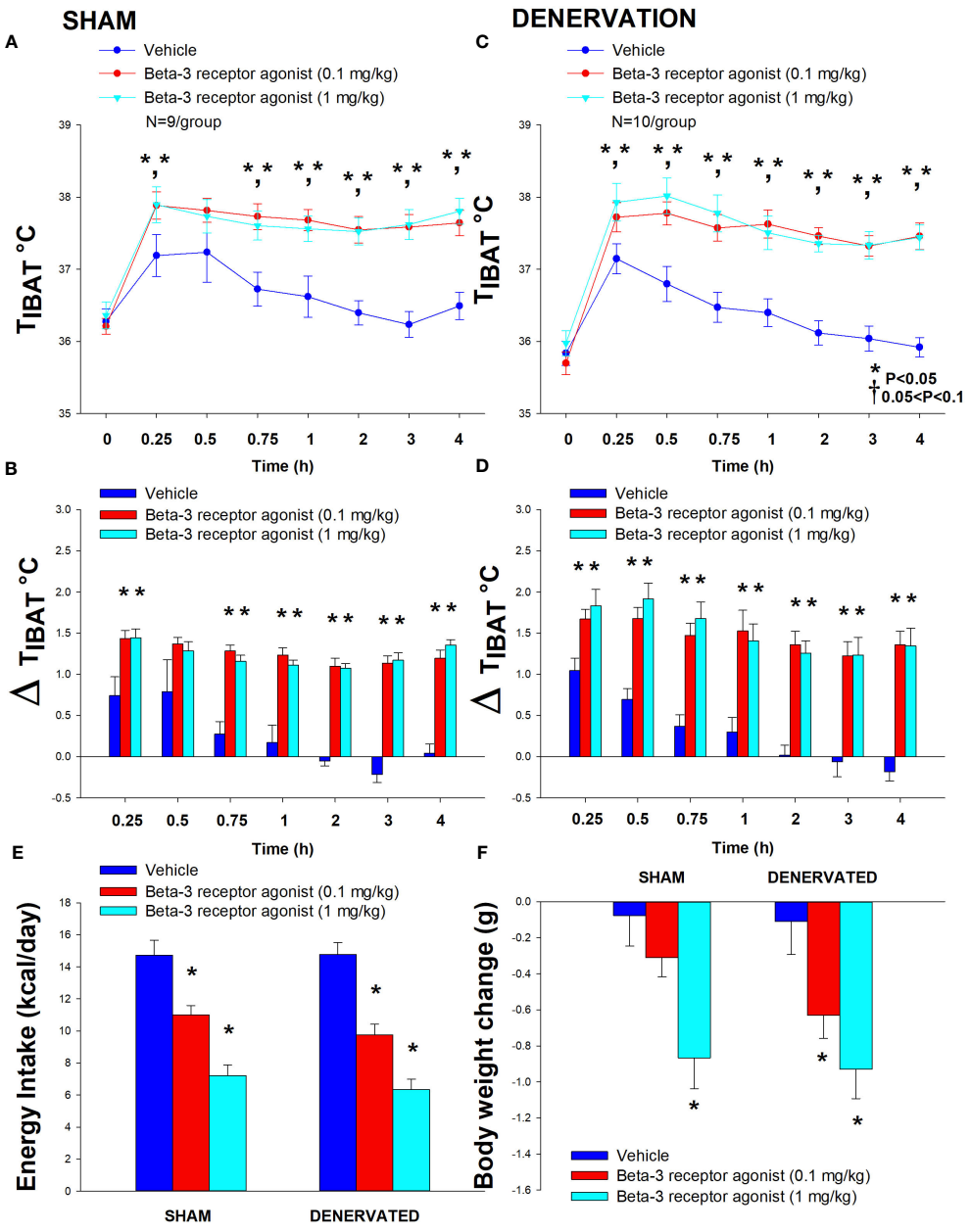

FIGURE 4
(A–F) Effect of systemic beta-3 receptor agonist (CL 316243) administration (0.1 and 1 mg/kg) on IBAT temperature (T_{IBAT}), energy intake and body weight post-sham or IBAT denervation in DIO mice. Mice were maintained on HFD (60% kcal from fat; N=9-10/group) for approximately 4.5 months prior to undergoing a sham or bilateral surgical IBAT denervation and implantation of temperature transponders underneath IBAT. Animals were subsequently adapted to a 4-h fast prior to receiving IP injections of (CL 316243) (0.1 or 1 mg/kg, IP) or vehicle (sterile water) where each animal received each treatment at approximately 7-day intervals. **(A, C)**, Effect of CL 316243 on T_{IBAT} in **(A)** sham operated or **(C)** IBAT denervated DIO mice; **(B, D)**, Effect of CL 316243 on change in T_{IBAT} relative to baseline T_{IBAT} (delta T_{IBAT}) in **(B)** sham operated or **(D)** IBAT denervated DIO mice; **(E)**, Effect of CL 316243 on change in energy intake in sham or IBAT denervated DIO mice; **(F)**, Effect of CL 316243 on change in body weight in sham or IBAT denervated DIO mice. Data are expressed as mean ± SEM. *P<0.05, †0.05<P<0.1 CL 316243 vs. vehicle.

(0.05<P<0.1; Figure 5C). Similar findings were apparent when measuring change in T_{IBAT} relative to baseline T_{IBAT} (Figure 5D). In addition, 4V OT elevated T_{IBAT} in lean denervated mice (data not shown).

There was no effect of acute 4V OT administration to reduce daily energy intake or body weight (P=NS) in either sham or denervated mice. Furthermore, there was no difference in energy intake [sham: 11.3 ± 1.2 kcal; denervation: 10.2 ± 1.9 kcal] or change in body weight [sham: 0.3± 0.1g; denervation: 0.4 ± 0.3 g] following acute 4V vehicle injections between sham or denervated mice (P=NS).

Overall, these findings demonstrate that SNS innervation of IBAT is not a predominant mediator of OT-elicited elevations of BAT thermogenesis.

In contrast to the pattern observed following 4V administration, systemic administration of OT produced an initial reduction of T_{IBAT} (P<0.05) followed by an increase in T_{IBAT} (P<0.05;

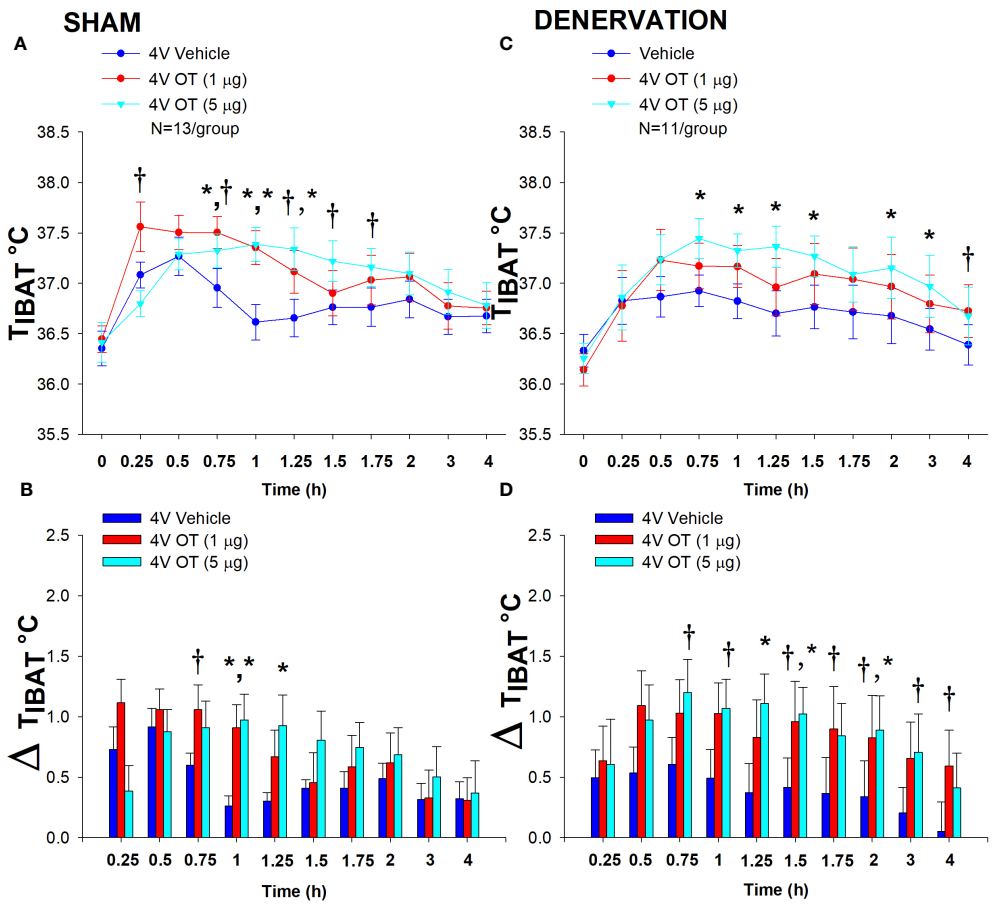

FIGURE 5
(A–D) Effect of acute 4V OT administration (1 and 5 µg) on T_{IBAT} post-sham or IBAT denervation in male DIO mice. Mice were maintained on HFD (60% kcal from fat; N=11-13/group) for approximately 4.25 months prior to undergoing a sham or bilateral surgical IBAT denervation and implantation of temperature transponders underneath IBAT. Mice were subsequently implanted with 4V cannulas and allowed to recover for 2 weeks prior to receiving acute 4V injections of OT or vehicle. Animals were subsequently adapted to a 4-h fast prior to receiving acute 4V injections of OT or vehicle **(A, C)**, Effect of acute 4V OT on T_{IBAT} in **(A)** sham operated or **(C)** IBAT denervated DIO mice; **(B, D)**, Effect of acute 4V OT on change in T_{IBAT} relative to baseline $T_{IBA}T$ (delta T_{IBAT}) in **(B)** sham operated or **(D)** IBAT denervated DIO mice; Data are expressed as mean ± SEM. *P<0.05, †0.05<P<0.1 OT vs. vehicle. The T_{IBAT} data from sham-operated DIO mice has been previously published (22).

Supplementary Figures 3A–D). Similar to OT, the melanocortin 3/4 receptor agonist, melanotan II (MTII), produced an initial reduction of T_{IBAT} (P<0.05; data not shown) followed by a subsequent increase in T_{IBAT} (data not shown; P<0.05).

Study 6A: determine the extent to which sympathetic outflow to IBAT contributes to the ability of OT to elicit weight loss in DIO mice

The goal of this study was to determine if OT-elicited weight loss requires intact SNS outflow to IBAT. By design, DIO mice were obese as determined by both body weight (47.9 ± 0.6 g) and adiposity (17.7 ± 0.5 g fat mass; 36.9 ± 0.7% adiposity) after maintenance on the HFD for approximately 4.25-4.5 months prior to sham/denervation procedures. There was no difference in body weight between sham and denervation groups prior to surgery (sham: 46.3 ± 1.0 g vs denervation: 47.9 ± 0.8 g) [(F(1,28) = 1.532, P=NS)].

IBAT NE content was reduced in denervated mice by 93.9 ± 2.3% in denervated mice relative to sham-operated control mice [(F(1,28) = 23.306, P=0.000). In contrast, there was no difference in NE content in IWAT, EWAT, liver or pancreas between sham or denervation groups (P=NS)

Chronic 4V OT reduced body weight by 5.7 ± 2.23% and 6.6 ± 1.4% in sham and denervated mice (P<0.05), respectively, and this effect was similar between groups (P=NS). OT produced corresponding reductions in fat mass (P<0.05) and this effect was also similar between groups (P=NS).

As expected, 4V vehicle resulted in 7.5 ± 3.0% weight gain relative to vehicle pre-treatment [(F(1,8) = 5.677, P=0.044)]. In contrast, 4V OT reduced body weight by 5.7 ± 2.23% relative to OT pre-treatment [(F(1,7) = 5.903, P=0.045)] (Figure 6A) and reduced weight gain (Figure 6B) between days 4-29 of the infusion period (P<0.05). 4V OT tended to reduce weight gain between days 2-3 (0.05<P<0.1). OT produced a corresponding reduction in fat mass [(F(1,13) = 5.190, P=0.040)] (Figure 6C) with no effect on lean body mass (P=NS). These effects were mediated, at least in part, by a modest reduction of

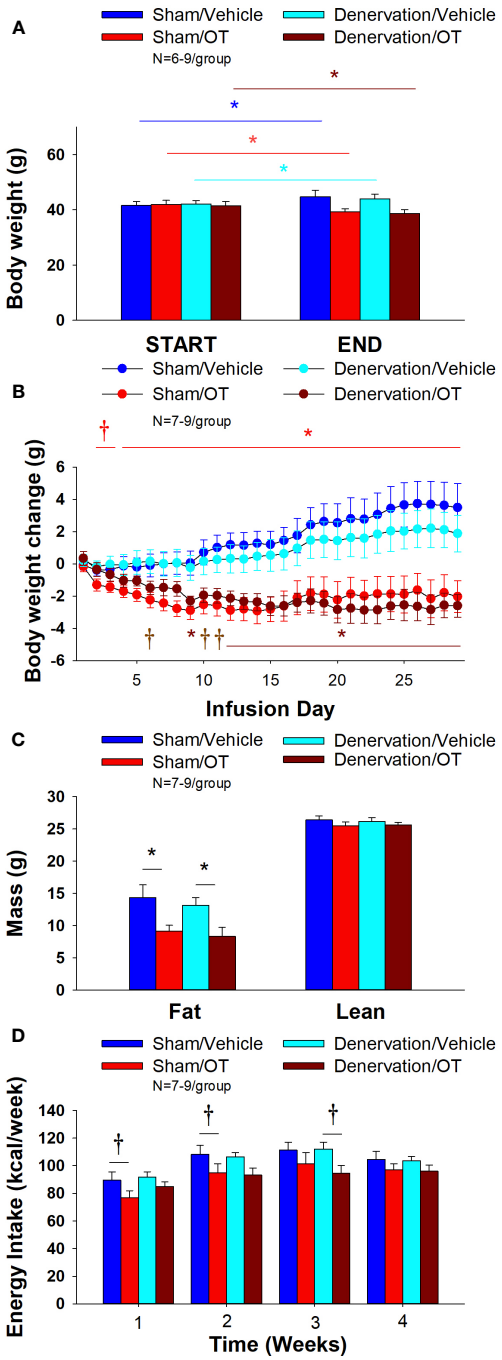

FIGURE 6
(A–D) Effect of chronic 4V OT infusions (16 nmol/day) on body weight, adiposity and energy intake post-sham or IBAT denervation in male DIO mice. **(A)**, Mice were maintained on HFD (60% kcal from fat; N=7-9/group) for approximately 4.25-4.5 months prior to undergoing a sham or bilateral surgical IBAT denervation. Mice were subsequently implanted with 4V cannulas and allowed to recover for 2 weeks prior to being implanted with subcutaneous minipumps that were subsequently attached to the 4V cannula. *A*, Effect of chronic 4V OT or vehicle on body weight in sham operated or IBAT denervated DIO mice; **(B)**, Effect of chronic 4V OT or vehicle on body weight change in sham operated or IBAT denervated DIO mice; **(C)**, Effect of chronic 4V OT or vehicle on adiposity in sham operated or IBAT denervated DIO mice; **(D)**, Effect of chronic 4V OT or vehicle on adiposity in sham operated or IBAT denervated DIO mice. Data are expressed as mean ± SEM. *P<0.05, †0.05<P<0.1 OT vs. vehicle.

energy intake that tended to be present during weeks 1 (P=0.067; Figure 6D) and 2 (P=0.092).

In denervated mice, 4V vehicle treatment resulted in 4.3 ± 2.6% weight gain relative to vehicle pre-treatment [(F(1,5) = 17.371, P=0.009)]. In contrast, 4V OT reduced body weight by 6.6 ± 1.4% relative to OT pre-treatment [(F(1,5) = 15.883, P=0.010)] (Figure 6A) and it reduced weight gain (Figure 6B) throughout the 29-day infusion period. OT treatment reduced weight gain on days 9 and 12-29 (P<0.05) and it tended to reduce weight gain on days 6 (P=0.095), 10 (P=0.059) and 11 (P=0.055). OT produced a

corresponding reduction in fat mass [(F(1,11) = 7.101, P=0.022)] (Figure 6C) with no effect on lean body mass (P=NS). These effects were mediated, at least in part, by a modest reduction of energy intake that tended to be present during weeks 2 (P=0.147) and 3 (P=0.064; Figure 6D).

Furthermore, there was no difference in total 4-week energy intake [sham: 413.5 ± 21.9 kcal; denervation: 414.1 ± 10.6 kcal] or 4-week change in body weight [sham: 3.6± 1.4 g; denervation: 2.1 ± 1.1 g] following chronic 4V vehicle infusion between sham or denervated mice (P=NS).

Based on these collective findings, we conclude that SNS innervation of IBAT is not a predominant contributor of oxytocin-elicited increases in BAT thermogenesis (surrogate measure of EE), weight loss and reduction of fat mass.

Adipocyte size

Sham

There was a significant effect of 4V OT to reduce EWAT adipocyte size in sham operated mice [(F(1,13) = 5.729, P=0.032)] (Figure 7B) while it had no significant effect on IWAT adipocyte size (P=NS) (Figure 7A).

Denervation

In contrast to the effects observed in sham mice, 4V OT had no significant effect on EWAT adipocyte size in IBAT denervated mice (P=NS) (Figure 7B). However, there was a tendency of 4V OT to reduce IWAT adipocyte size in IBAT denervated mice [(F(1,11) = 4.233, P=0.064)] (Figure 7A).

Plasma hormone concentrations

To characterize the endocrine and metabolic effects between sham and denervated DIO mice, we measured blood glucose levels and plasma concentrations of leptin, insulin, FGF-21, irisin, adiponectin, FFA, free glycerol (FG) and total cholesterol (TC) post-sham and denervation procedure. We found an overall effect of 4V OT to reduce plasma leptin [(F(3,26) = 3.839, P=0.021)]. Specifically, 4V OT treatment was associated with a reduction of plasma leptin in the sham group (P<0.05; Table 2) which coincided with OT-elicited reductions in fat mass. We also found that 4V OT treatment tended to reduce plasma insulin in the denervation group relative to the 4V vehicle sham group (P=0.081; Table 2). In addition, there was an overall effect of OT to reduce plasma total cholesterol [(F(3,26) = 5.806, P=0.004)]. 4V OT treatment was associated with a significant reduction of total cholesterol in both groups (P<0.05; Table 2).

Study 6B: determine the extent to which sympathetic outflow to IBAT contributes to the ability of OT to impact thermogenic gene expression in IBAT, IWAT and EWAT in DIO mice

IBAT

There was a reduction of IBAT UCP-1 [(F(1,7) = 38.1, P<0.001)], DIO2 [(F(1,7) = 12.669, P=0.009)], Gpr120 [(F(1,7) = 65.965, P<0.001)], Adrb3 [(F(1,7) = 65.916, P=0.000)], Adrb1 [(F(1,7) = 8.015, P=0.025)], Acox1 [(F(1,7) = 58.261, P<0.001)], bmp8b [(F(1,7) = 19.636, P=0.003)], cox8b [(F(1,6) = 16.403, P=0.007)] and UCP-3 mRNA expression [(F(1,7) = 57.665, P<0.001)] in denervated mice relative to IBAT from sham operated mice (P<0.05; Table 3A). There were no significant differences in IBAT CIDEA, PPARGC1, PPARA and PRDM16 mRNA expression between sham and denervation groups (P=NS).

The findings pertaining to IBAT UCP-1 gene expression in surgically denervated mice are consistent with what others have reported with IBAT UCP-1 protein expression from hamsters (51) and mice (52) following chemical (6-OHDA)-induced denervation of IBAT relative to control animals. Similarly, there was a reduction of IBAT UCP-1 mRNA following unilateral or bilateral surgical denervation in hamsters (53) and mice (54, 55), respectively. Similar to our findings, others also found a reduction of IBAT Dio2 and Adrb3 following bilateral surgical denervation in mice (54). The findings pertaining to IBAT UCP-1 gene expression in denervated mice are consistent with what others have reported with IBAT UCP-1 protein expression from hamsters (51) and mice (52) with chemical (6-OHDA)-induced denervation of IBAT relative to control animals.

IWAT

IWAT UCP-1 [(F(1,2) = 11.131, P=0.079)] tended to be elevated in denervated mice relative to sham operated mice (Table 3B). There were no significant differences in any of the other thermogenic markers (P=NS; Table 3B).

EWAT

There tended to be a reduction of UCP-1 in denervated mice compared to sham operated mice [(F(1,2) = 7.000, P=0.118)] (Table 3C). There were no significant differences in any of the other thermogenic markers (P=NS; Table 3C).

Study 7: determine the extent to which systemic (subcutaneous) infusion of a centrally effective dose of OT (16 nmol/day) elicits weight loss in DIO mice

As expected, weight gain of DIO mice increased over the month of vehicle treatment relative to pre-treatment [(F(1,10) = 16.901, P=0.002)] (Figure 8A). In contrast to the weight lowering effects of 4V OT (16 nmol/day), systemic OT (16 nmol/day) resulted in a significant elevation of body weight relative to OT pre-treatment [(F(1,12) = 11.138, P=0.006)] (Figure 8A; P<0.05). Furthermore, SC OT, at a 3-fold higher dose (50 nmol/day), also resulted in a significant elevation of body weight relative to pre-treatment [(F(1,12) = 10.424, P=0.007)]. However, SC OT (16 and 50 nmol/day) was able to reduce weight gain (Figure 8B) relative to vehicle treatment throughout the 28-day infusion period. SC OT (50 nmol/day), at a dose that was at least 3-fold higher than the centrally effective dose (16 nmol/day), reduced weight gain throughout the entire 28-day infusion period. SC OT (16 nmol/day) treated mice had reduced weight gain between days 17-28 (P<0.05) but did not have the net weight loss seen when this dose

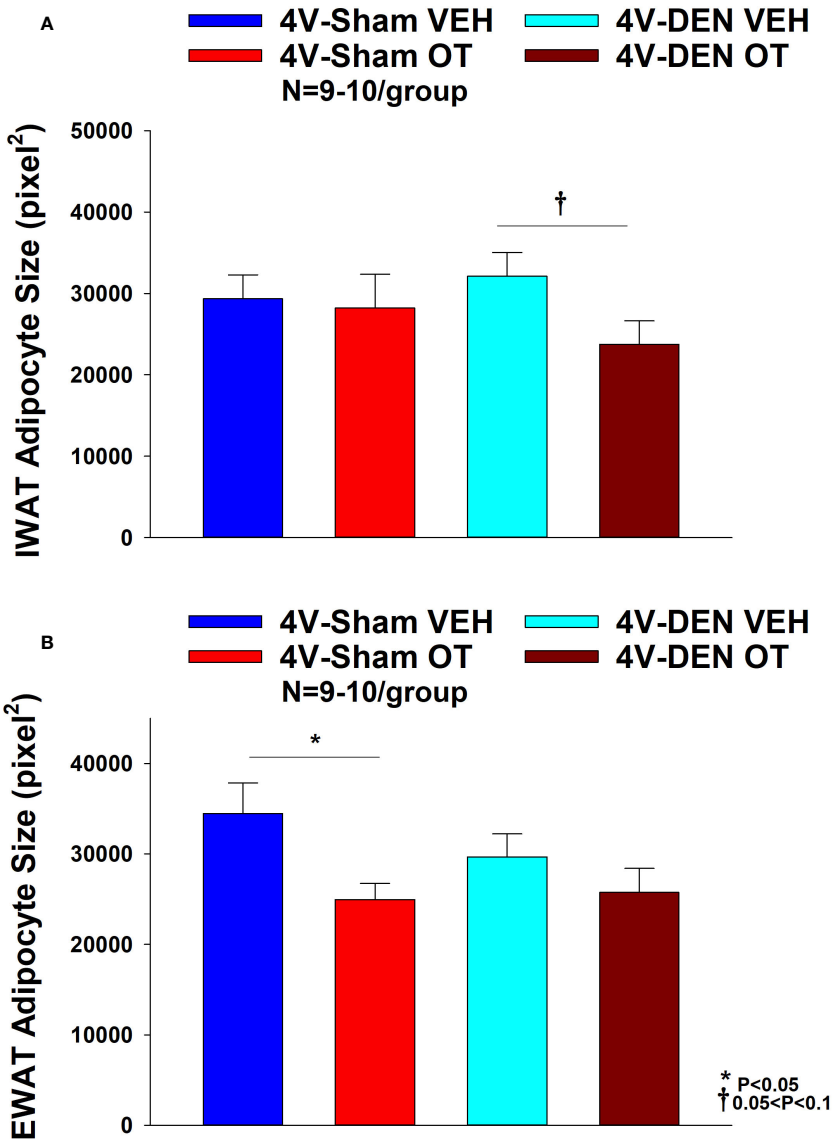

FIGURE 7
(A, B) Effect of chronic 4V OT infusions (16 nmol/day) on adipocyte size post-sham or IBAT denervation in male DIO mice. **(A)**, Adipocyte size (pixel^2) was measured in IWAT from mice that received chronic 4V infusion of OT (16 nmol/day) or vehicle (VEH) in sham or IBAT denervated DIO mice (N=9-10/group). **(B)**, Adipocyte size was measured in EWAT from mice that received chronic 4V infusion of OT (16 nmol/day) or vehicle in sham operated or IBAT denervated mice (N=9-10/group). Data are expressed as mean ± SEM. *P<0.05 OT vs. vehicle.

was given centrally. SC OT (16 and 50 nmol/day) reduced fat mass [(F(2,35) = 5.558, P=0.008)] (Figure 8C; P<0.05) and produced a corresponding reduction of plasma leptin [(F(2,35) = 3.890, P=0.03)], (Table 4) with no effect on lean body mass (P=NS). These effects that were mediated, at least in part, by a modest reduction of energy intake that was apparent during week 3 of SC OT (50 nmol/day) treatment (Figure 8D; P<0.05).

Discussion

The goal of the current studies was to determine if sympathetic innervation of IBAT is required for OT to increase non-shivering BAT thermogenesis and reduce body weight and adiposity in male DIO mice. To assess if OT-elicited changes in non-shivering BAT thermogenesis require intact SNS outflow to IBAT, we examined the effects of acute 4V OT (1, 5 µg) on T_{IBAT} in DIO mice following bilateral surgical SNS denervation to IBAT. We found that the high dose (5 µg) elevated T_{IBAT} similarly in sham mice as in denervated mice. We subsequently determined if OT-elicited reductions of body weight and adiposity require intact SNS outflow to IBAT. To accomplish this, we determined the effect of bilateral surgical denervation of IBAT on the ability of chronic 4V OT (16 nmol/day) administration to reduce body weight, adiposity and food intake in DIO mice. We found that chronic 4V OT produced comparable reductions of body weight and adiposity in denervated mice, as well as sham mice (P<0.05), supporting the hypothesis that sympathetic innervation of IBAT is not a predominant mediator of

TABLE 2 Plasma Measurements Following 4V Infusions of Oxytocin or Vehicle in Sham and Denervated DIO Mice.

4V Treatment	Vehicle	OT	Vehicle	OT
	Sham	Sham	Denervation	Denervation
Leptin (ng/mL)	36.5 ± 9.7[a]	13.4 ± 2.6[b]	23.1 ± 2.9[a]	9.7 ± 2.3[ab]
Insulin (ng/mL)	2.5 ± 0.5[a]	1.6 ± 0.2[ab]	1.8 ± 0.2[ab]	1.4 ± 0.3[bc]
FGF-21 (pg/mL)	856.4 ± 172[a]	679 ± 57.3[a]	698.4 ± 87.1[a]	505.5 ± 112.2[a]
Irisin (μg/mL)	3.3 ± 0.7[a]	2.6 ± 0.3[a]	3.1 ± 0.6[a]	2.0 ± 0.1[a]
Adiponectin (μg/mL)	11.3 ± 1.2[a]	10.0 ± 1.0[a]	14.0 ± 2.1[a]	12.1 ± 2.7[a]
Blood Glucose (mg/dL)	169.5 ± 5.5	156.6 ± 4.8	168.6 ± 5.6	158.3 ± 8.3
FFA (mEq/L)	0.5 ± 0.02[a]	0.5 ± 0.04[a]	0.5 ± 0.02[a]	0.6 ± 0.09[a]
Free Glycerol (mg/dL)	40.3 ± 1.7[a]	42.1 ± 1.9[a]	44.6 ± 2.3[a]	40.5 ± 3.9[a]
Total Cholesterol (mg/dL)	253.9 ± 7.4[a]	214.2 ± 12.6[b]	229.6 ± 7.8[a]	198.3 ± 10.9[b]

Blood was collected by tail vein nick (blood glucose) or from the trunk following a 4-h fast.
Different letters denote significant differences between treatments.
Shared letters are not significantly different from one another.
Data are expressed as mean ± SEM.
N=6-9/group.

OT-elicited increases of non-shivering BAT thermogenesis and reductions of body weight and adiposity in male DIO mice.

Our finding that OT produced these effects when given into the hindbrain (4V) suggest that hindbrain populations and/or spinal cord populations may contribute to the effects of OT-elicited thermogenesis and browning of WAT in mice. Recent findings highlight the presence of both overlapping and nonoverlapping CNS circuits that control SNS outflow to IWAT and IBAT (51). Namely, parvocellular PVN OT neurons have multi-synaptic projections to IBAT (59, 60), IWAT (59, 61) and EWAT (61, 62). A small subset of parvocellular PVN OT neurons overlap and project to both IBAT and IWAT (59). OT neurons are anatomically situated to control SNS outflow to IBAT and IWAT and increase BAT thermogenesis and browning of IWAT, respectively. It is not clear if these effects are mediated by the same OT neurons or through distinct OT neurons that project to the hindbrain nucleus of the solitary tract or nucleus tractus solitarius (NTS) (63, 64) and/or spinal cord (64), both of which are sites that can control SNS outflow to IBAT and BAT thermogenesis (65, 66). Ong and colleagues recently found that viral-elicited knockdown of OTR mRNA within the dorsal vagal complex was unable to block the effects of 4V OT to increase core temperature (67) suggesting that other OTRs within other areas of the hindbrain and/or spinal cord may contribute to these effects in a rat model. It will be important to determine whether 4V OT-elicited BAT thermogenesis is mediated by OTRs within regions of the NTS not targeted by Ong and colleagues (67), other hindbrain areas such as the raphe pallidus (29, 66, 68–70) or spinal cord (23).

One outstanding question is how 4V OT is activating IBAT if not through SNS outflow to IBAT. Our findings that 1) systemic administration of OT, at a dose that stimulated T_{IBAT} when given into the 4V, did not fully recapitulate the temporal profile we found following 4V administration and 2) 4V administration failed to reproduce the reduction of T_{IBAT} observed following systemic administration suggest that 4V OT is not likely leaking into the periphery to act at peripheral OTRs. One possibility might be that 4V OT activates OTRs within the hindbrain and/or spinal cord that results in the stimulation of epinephrine from the adrenal gland and subsequent activation of IBAT. Epinephrine has been previously found to stimulate both lipolysis and respiration from brown adipocytes derived from rat IBAT (71) and it has only a 2.5-fold lower affinity for recombinant β3-AR in CHO cells than NE (72). In addition, mice that lack epinephrine are able to maintain body temperature in response to cold stress but fail to show an increase in IBAT UCP-1 or PGC1-alpha (73) suggesting that non-UCP mechanisms may be involved to increase or retain heat. However, while it is clear that the hindbrain and spinal cord are part of a multi-synaptic projection to the adrenal gland (74, 75), only 1% of PVN OT neurons within either the parvocellular PVN or magnocellular PVN were found to have multi-synaptic projections to the adrenal gland (74). Whether 4V OT activates a hindbrain or spinal cord projection to the adrenal gland resulting in the release of epinephrine and subsequent activation of IBAT will need to be examined in future studies.

One other possibility is that acute 4V OT could be activating IBAT secondary to stimulating locomotor activity. We have found the high dose (5 μg) given acutely into the 4V stimulated IBAT temperature (21) at doses that increased gross motor activity in DIO rats during the first 2-h post-injection ($P<0.05$; unpublished findings). In addition, Sakamoto and colleagues found that intracerebroventricular (ICV) administration of OT (0.5 μg) stimulated activity levels in mice (76). Similarly, Noble and colleagues found that acute ventromedial hypothalamic injections of OT (1 nmol ≈ 1.0072 μg) also stimulated short-term physical activity at 1-h post-injection in rats (12). Sutton and colleagues also reported that acute DREADD-elicited stimulation of OT neurons within the PVN produced an increase in locomotor activity, energy expenditure and subcutaneous IBAT temperature (23) in Oxytocin IRES-Cre mice whose transponders were placed above the IBAT

10.3389/fendo.2024.1440070

TABLE 3A Changes in mRNA Expression Following 4V Infusions of OT or VEH in Male DIO Mice.

4V Treatment	VEH	OT	VEH	OT
	Sham	Sham	Denervation	Denervation
IBAT				
Adrb1	1.0 ± 0.1^{a}	0.7 ± 0.1^{ab}	0.5 ± 0.1^{b}	1.5 ± 0.5^{c}
Adrb3	1.0 ± 0.1^{a}	0.7 ± 0.2^{ab}	0.3 ± 0.1^{b}	0.9 ± 0.2^{a}
Acox1	1.0 ± 0.1^{a}	1.2 ± 0.3^{a}	0.4 ± 0.1^{b}	0.2 ± 0.1^{b}
UCP1	1.0 ± 0.3^{a}	0.8 ± 0.2^{ab}	0.1 ± 0.01^{b}	0.6 ± 0.5^{ab}
UCP3	1.0 ± 0.1^{ab}	1.4 ± 0.5^{a}	0.2 ± 0.1^{b}	0.3 ± 0.1^{b}
Cidea	1.0 ± 0.1^{a}	0.8 ± 0.2^{a}	0.3 ± 0.1^{b}	0.3 ± 0.1^{b}
Cox8b	1.0 ± 0.1^{a}	1.0 ± 0.1^{a}	0.2 ± 0.1^{b}	0.5 ± 0.1^{b}
DIO2	1.0 ± 0.2^{a}	0.6 ± 0.1^{b}	0.1 ± 0.1^{c}	1.2 ± 0.1^{a}
Ppara	1.0 ± 0.1^{a,b}	1.7 ± 0.6^{a}	0.5 ± 0.1^{b}	0.2 ± 0.1^{b}

IBAT was collected following a 4-h fast.
Different letters denote significant differences between treatments.
Shared letters are not significantly different from one another.
Data are expressed as mean ± SEM.
N=3-8/group.

TABLE 3B Changes in mRNA Expression Following Acute 4V OT or VEH Injections in Male DIO Mice.

4V Treatment	VEH	OT	VEH	OT
	Sham	Sham	Denervation	Denervation
IWAT				
Adra2a	1.0 ± 0.2^{a}	2.1 ± 1.0^{a}	0.8 ± 0.2^{a}	0.9 ± 0.3^{a}
Adrb3	1.0 ± 0.1^{a}	1.8 ± 0.5^{a}	1.7 ± 0.6^{a}	2.1 ± 0.7^{a}
Acox1	1.0 ± 0.3^{a}	0.7 ± 0.2^{a}	1.3 ± 0.2^{a}	1.3 ± 0.2^{a}
UCP1	1.0 ± 0.4^{ab}	1.4 ± 0.7^{a,b}	0.6 ± 0.1^{a}	2.9 ± 0.9^{bc}
DIO2	1.0 ± 0.3^{a}	0.2 ± 0.1^{a}	0.6 ± 0.1^{a}	1.3 ± 1.0^{a}
Ppara	1.0 ± 0.2^{a}	0.8 ± 0.3^{a}	1.5 ± 0.4^{a}	1.7 ± 0.2^{a}

IWAT was collected following a 4-h fast.
Different letters denote significant differences between treatments.
Shared letters are not significantly different from one another.
Data are expressed as mean ± SEM.
N=3-7/group.

TABLE 3C Changes in mRNA Expression Following Acute 4V OT or VEH Injections in Male DIO Mice.

4V Treatment	VEH	OT	VEH	OT
	Sham	Sham	Denervation	Denervation
EWAT				
Adra2a	1.0 ± 0.5^{a}	0.4 ± 0.1^{a}	1.1 ± 0.4^{a}	0.8 ± 0.2^{a}
Adrb3	1.0 ± 0.3^{a}	4.1 ± 1.2^{b}	0.4 ± 0.1^{a}	3.4 ± 1.3^{a,b}
Acox1	1.0 ± 0.1^{a,b}	1.1 ± 0.1^{a,b}	0.7 ± 0.2^{a}	1.4 ± 0.1^{b}
DIO2	1.0 ± 0.3^{a}	0.7 ± 0.1^{a}	0.6 ± 0.4^{a}	1.7 ± 0.8^{a}

EWAT was collected following a 4-h fast.
Different letters denote significant differences between treatments.
Shared letters are not significantly different from one another.
Data are expressed as mean ± SEM.
N=3-5/group.

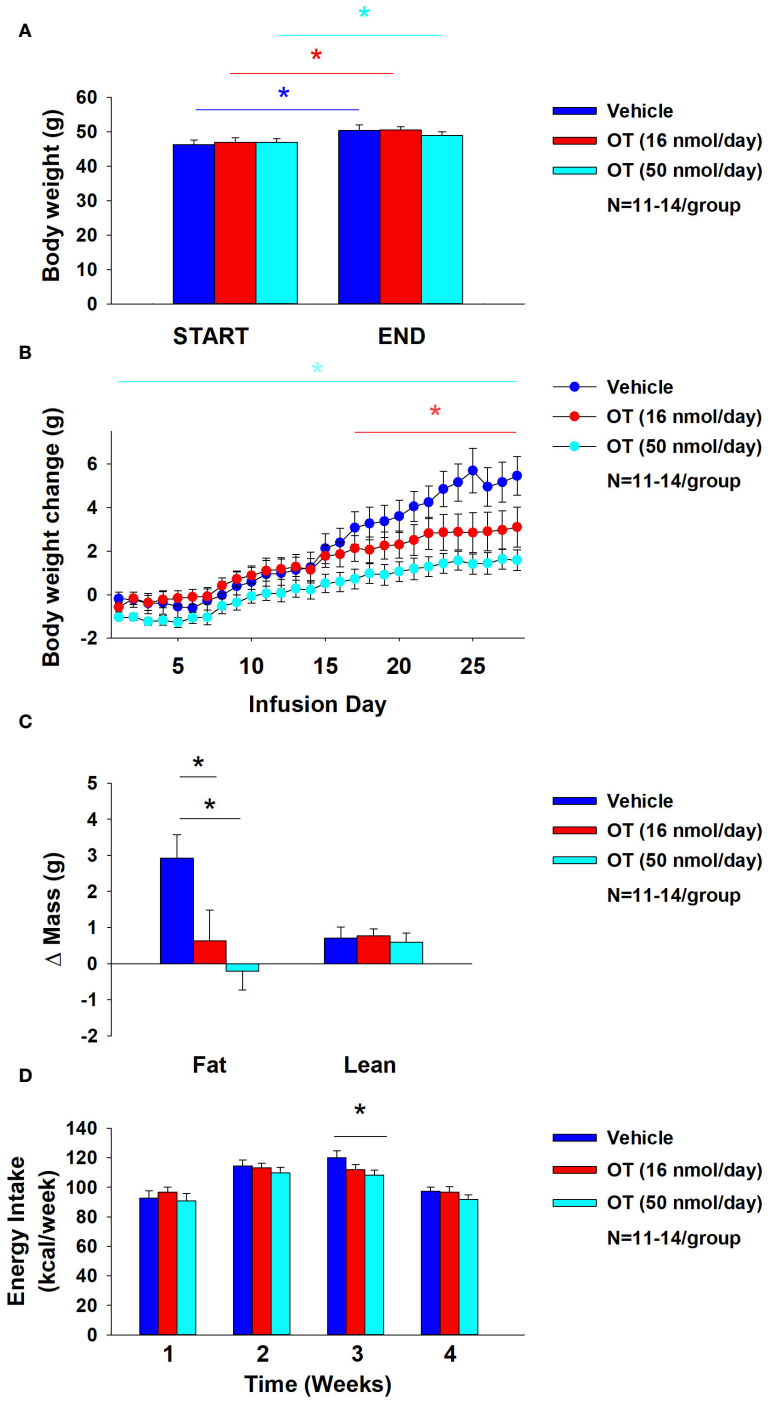

FIGURE 8
(A–D) Effect of chronic subcutaneous OT infusions (16 and 50 nmol/day) on body weight, adiposity and energy intake in male DIO mice. **(A)**, Mice were maintained on HFD (60% kcal from fat; N=11-14/group) for approximately 4-4.25 months prior to being implanted with temperature transponders and allowed to recover for 1-2 weeks prior to being implanted with subcutaneous minipumps. **(A)**, Effect of chronic subcutaneous OT or vehicle on body weight in DIO mice; **(B)**, Effect of chronic subcutaneous OT or vehicle on body weight change in DIO mice; **(C)**, Effect of chronic subcutaneous OT or vehicle on adiposity in DIO mice; **(D)**, Effect of chronic subcutaneous OT or vehicle on adiposity in DIO mice. Data are expressed as mean ± SEM. *P<0.05, †0.05<P<0.1 OT vs. vehicle.

pad. This finding raises that possibility that endogenous OT may also elicit increases in activity. Studies aimed at blocking endogenous OTR signaling prior to DREADD activation of PVN OT neurons will help determine the extent to which these effects are mediated by OT. Future studies will be required in order to examine the extent to which locomotor activity may contribute to the effects of acute 4V on T_{IBAT} in DIO mice

Recent findings also implicate a potentially important role of peripheral OT receptors in the control of body weight in rodents. Similar to our studies, Yuan and colleagues found systemic OT (100

10.3389/fendo.2024.1440070

TABLE 4 Plasma measurements following SC infusions of oxytocin or vehicle in DIO mice.

SC Treatment	Vehicle	OT (16 nmol/day)	OT (50 nmol/day)
Leptin (ng/mL)	90.4 ± 7.8[a]	68 ± 3.6[b]	69.9 ± 6.5[b]
FGF-21 (pg/mL)	2387.3 ± 250[a]	3087.4 ± 414.2[a]	3084.1 ± 520[a]
Irisin (μg/mL)	3.5 ± 0.3[a]	3.7 ± 0.3[a]	4.2 ± 0.4[a]
Adiponectin (μg/mL)	14.1 ± 0.7[a]	11.4 ± 1.0[b]	12.1 ± 0.9[ab]
Blood Glucose (mg/dL)	226.5 ± 12.2[a]	234.5 ± 12.7[a]	209.3 ± 11.0[a]
FFA (mEq/L)	0.1 ± 0.02[a]	0.1 ± 0.01[a]	0.1 ± 0.01[a]
Glycerol (mg/dL)	20.2 ± 0.7[a]	23.8 ± 1.5[a]	20.3 ± 1.8[a]
Total Cholesterol (mg/dL)	242.5 ± 7.2[a]	227.7 ± 9.4[a]	227.3 ± 9.2[a]

Blood was collected by tail vein nick (blood glucose) or from the trunk following a 4-h fast.
Different letters denote significant differences between treatments.
Shared letters are not significantly different from one another.
Data are expressed as mean ± SEM.
N=11-14/group.

nmol/day ≈ 100.72 μg/day) reduced weight gain in high fat diet-fed mice and these effects were associated with decreased adipocyte size (IWAT and EWAT). Asker and colleagues extended these findings and reported that a novel BBB-impermeable OT analog, OT-B12, reduced food intake in rats, thus providing additional evidence for the importance of peripheral OTRs in the control of food intake (77). These findings are in line with earlier studies by Iwasaki and colleagues who found that the effects of peripheral OT to reduce food intake were attenuated in vagotomized mice (78, 79). Similarly, previous findings from our lab also indicated that peripheral administration of a non-BBB penetrant OTR antagonist, L-371257, resulted in a modest stimulation of food intake and body weight gain in rats (80). These findings suggest that, in addition to a central mechanism mediated through hindbrain and/or spinal cord OTRs, OT may also act peripherally to reduce adipocyte size through a direct action on OTRs found on adipocytes (9, 81, 82).

The role of peripheral OTR in the control of BAT thermogenesis is not entirely clear but recent studies raise the possibility that systemic OT may impact BAT thermogenesis through a direct mechanism. Yuan and colleagues found that slow continuous systemic infusion of OT (100 nmol/day) elevated rectal temperature (single time point), UCP-1 protein and UCP-1 mRNA in IBAT and IWAT of high fat diet-fed mice (24) where OTR are expressed (24). In contrast, we found that a single acute bolus injection of lower doses of OT (5 and 10 μg/μL) elicited an initial reduction of T_{IBAT} prior to a subsequent elevation of T_{IBAT}. Similarly, others have found that peripheral administration of higher doses of OT (1 mg/kg) elicited a robust hypothermic response (83). Similar doses (1, 3 and 10 mg/kg, IP) were also found to block stress-induced stimulation of core temperature (84). Kohli reported that pretreatment with arginine vasopressin receptor 1A (AVPR1A) antagonist can reduce OT-mediated hypothermia, while pretreatment with OTR antagonist does not (85). Similar to systemic OT, we and others have demonstrated that systemic MTII produces an initial reduction of T_{IBAT} and/or core temperature (86, 87) followed by a subsequent elevation of T_{IBAT} or core temperature (87). Like OT, MTII-elicited reduction of body temperature was found to be blunted in response to the AVPR1A antagonist (86). In addition to a mechanism involving AVPV1A, MTII-elicited hypothermia is also due, in part, to mast cell activation (88). Together, these findings suggest that the hypothermia in response to high doses of systemic OT might be mediated, in part, by arginine vasopressin (AVP) receptor V1A rather than through OTR. It remains to be determined whether the hypothermic effects of systemic OT are also mediated, in part, by activation of mast cells.

To our knowledge, this is the first time that SNS innervation of IBAT (NE content) has been found to be reduced in DIO rodents relative to age-matched lean control mice. These findings are consistent with the reduction of IBAT NE content in obese *fa/fa* Zucker rats relative to lean homo- (*Fa/Fa*) or heterozygous (*Fa/fa*) rats (89). Similarly, tyrosine hydroxylase (TH; rate limiting enzyme to synthesis of catecholamines) was found to be reduced in obese relative to lean animals (90). The same group also found a reduction of IBAT NE content, NE turnover and activity of dopamine-β-hydroxylase (rate limiting enzyme to synthesis of NE) in young *fa/fa* Zucker rats prior to obesity onset (91). Previous studies have found that the IBAT from humans with obesity appears to be hypoactive (92, 93) although it isn't clear if this is due to reduced SNS innervation of IBAT or reduced sensitivity to endogenous catecholamines (94). Consistent with these findings, obese offspring also show reductions of IBAT temperature (95). Defects in BAT activity are associated with impairments of both the structure and function of BAT mitochondria (96). Furthermore, the IBAT of obese animals was associated with enlarged lipid droplets (97), indicative of hypoactivity of IBAT. Together, our data support the hypothesis that impaired activation of IBAT in the context of DIO may be due, in part, to reduced SNS innervation of IBAT.

Our findings showing a reduction of IBAT UCP-1, Dio2, and Adbr3 in denervated mice is consistent with what has been reported from IBAT of denervated mice or hamsters (51–55). In addition, we found a reduction of IBAT Adrb1, Acox1, UCP-3, bmp8b, Gpr120, and Cox8b in denervated mice. We also found that 4V OT blocked the reduction of Adrb1, Adrb3 and Dio2 in IBAT of denervated mice. Whether these genes contributed to the ability of OT to increase T_{IBAT} in denervated mice is unclear. What was also unexpected was that the β3-AR agonist, CL 316243, was able to produce comparable effects on T_{IBAT} in both groups of mice despite there being a reduction of IBAT Adrb3. However, we have found that chronic 1x daily administration of CL 316243 produced similar effects on stimulation of T_{IBAT} on treatment day 1 vs day 19 despite there being a reduction of IBAT Adrb3 mRNA at the end of the study (98). It is possible that the presence of even a reduced level of the β3-AR in IBAT is sufficient to contribute to the effects of CL 316243 on IBAT temperature at the pharmacological doses used in our studies. It is not as likely that the effects of CL 316243 on IBAT temperature in denervated mice was due to action at other adrenergic receptors in IBAT because CL 316243 is highly

selective to the β3-AR [128-fold higher selectivity to human β3-AR vs β1-AR (99)]. Furthermore, CL 316,243 appears to be more selective to the mouse β3-AR relative to the human β3-AR based on stimulation of cAMP formation in transfected CHO cells (pEC_{50} 8.7 vs. 4.3) (100). In addition, CL 316243 is ineffective at increasing free fatty acids, insulin secretion, energy expenditure, and reducing food intake in β3-AR deficient mice (101) indicating that these effects of CL 316243 are mediated by β3-AR. Furthermore, the effects of CL 316243 on oxygen consumption, insulin secretion and food intake were completely restored with re-expression of β3-AR in brown and white adipocytes (102) indicating that these CL 316243-elicited effects are mediated by β3-AR specifically in BAT and/or WAT.

One limitation of our study is that restraint stress may have limited our ability to observe larger effects on T_{IBAT} (103) during the time period when the effect of the drug is relatively short-lived or small. We aimed to minimize the impact of restraint stress by adapting the animals to handling and mock injections during the week prior to the experiment and by administering the drugs during the early part of the light cycle when catecholamine levels (36) and IBAT temperature are lower (22). Despite these adjustments to protocol, we failed to observe an obvious impairment in the ability of the sympathomimetic, tyramine, to stimulate T_{IBAT} in denervated mice even though there was clear evidence that IBAT NE content was lower in mice whose IBAT was denervated. While the effects of OT and CL 316243 continued well beyond the short-lived effects of restraint/vehicle stress on T_{IBAT} in our mouse studies (~30-45 minutes), the effects of tyramine were relatively short-lived and may have been masked by restraint stress. Thus, stress-induced epinephrine, from the adrenal medulla, or global release of NE from SNS nerve terminals (in response to tyramine) (104–106), may have activated β3-AR in IBAT to stimulate T_{IBAT}, even in denervated mice.

We also acknowledge that the focus of this study was on IBAT given that IBAT is most well characterized BAT depot "because of its size, accessibility and clear innervation IBAT" (107). However, IBAT is thought to contribute to approximately 45% of total thermogenic capacity of BAT (54) or ≥ 70% of total BAT mass (108). Thus, it is possible that the other BAT depots (axillary, cervical, mediastinal and perirenal depots), all of which show elevated UCP-1 in response to cold (109), might have contributed to the effects of OT to elicit weight loss in IBAT denervated mice. Moreover, we acknowledge the potential contribution of IWAT and EWAT given that chronic 4V OT was able to elevate IWAT UCP-1 and EWAT Acox1 in a limited number of IBAT denervated mice. As mentioned earlier, previous findings demonstrate crosstalk between SNS circuits that innervate IBAT and WAT (51). In addition, there is increased NE turnover and IWAT UCP-1 mRNA expression in IBAT denervated hamsters (51). It will be important to 1) confirm our IWAT and WAT gene expression findings in a larger group of animals and 2) develop a model to assess the effectiveness of denervation of all BAT and specific WAT depots in order to more fully understand the importance of BAT and WAT depots in contributing to the effects of OT to elicit weight loss in rodent models.

In summary, our findings demonstrate that acute 4V OT (5 μg) produced comparable increases in T_{IBAT} in both denervated and sham mice. We subsequently found that chronic 4V OT produced similar reductions of body weight and adiposity in both sham and denervated mice. Importantly, our findings suggest that there is no change or obvious functional impairment in the response of the β3-AR agonist, CL 316243, to activate IBAT in mice with impaired SNS innervation of IBAT in comparison to sham-operated mice. Together, these findings support the hypothesis that sympathetic innervation of IBAT is not a predominant mediator of OT-elicited increases in non-shivering BAT thermogenesis and reductions of body weight and adiposity in male DIO mice.

Data availability statement

All relevant data is contained within the article: The original contributions presented in the study are included in the article/Supplementary Material, further inquiries can be directed to the corresponding author/s.

Ethics statement

The animal study was approved by VA Puget Sound Health Care System IACUC. The study was conducted in accordance with the local legislation and institutional requirements.

Author contributions

ME: Conceptualization, Data curation, Investigation, Methodology, Project administration, Supervision, Writing – review & editing. HN: Conceptualization, Data curation, Formal analysis, Investigation, Methodology, Project administration, Validation, Writing – review & editing. AD: Conceptualization, Data curation, Formal analysis, Investigation, Methodology, Project administration, Validation, Writing – review & editing. AH: Data curation, Formal analysis, Investigation, Methodology, Project administration, Writing – review & editing. TW-H: Data curation, Formal analysis, Investigation, Methodology, Project administration, Validation, Writing – review & editing. TW: Data curation, Formal analysis, Investigation, Methodology, Writing – review & editing. MH: Data curation, Formal analysis, Investigation, Methodology, Project administration, Supervision, Validation, Writing – review & editing. JS: Data curation, Formal analysis, Investigation, Methodology, Project administration, Supervision, Validation, Writing – review & editing. KO'b: Data curation, Formal analysis, Methodology, Project administration, Supervision, Writing – review & editing. JG: Data curation, Formal analysis, Investigation, Methodology, Project administration, Validation, Writing – review & editing. PH: Conceptualization, Data curation, Formal analysis, Methodology, Project administration, Resources, Supervision, Validation, Writing – review & editing. TM: Methodology, Project administration, Supervision, Validation, Writing – original draft, Writing – review & editing. CS: Data curation, Formal

analysis, Investigation, Methodology, Validation, Writing – review & editing. EP: Project administration, Resources, Supervision, Validation, Writing – review & editing. VR: Methodology, Supervision, Validation, Writing – review & editing. GT: Conceptualization, Methodology, Supervision, Validation, Writing – original draft, Writing – review & editing. JB: Conceptualization, Data curation, Formal analysis, Funding acquisition, Investigation, Methodology, Project administration, Resources, Supervision, Validation, Writing – original draft, Writing – review & editing.

Funding

The author(s) declare financial support was received for the research, authorship, and/or publication of this article. This material was based upon work supported by the Office of Research and Development, Medical Research Service, Department of Veterans Affairs (VA) and the VA Puget Sound Health Care System Rodent Metabolic Phenotyping Core and the Cellular and Molecular Imaging Core of the Diabetes Research Center at the University of Washington and supported by National Institutes of Health (NIH) grant P30DK017047. This work was also supported by the VA Merit Review Award 5 I01BX004102 (JB), from the United States (U.S.) Department of Veterans Affairs Biomedical Laboratory Research and Development Service. Research reported in this publication is a project of the Seattle Institute for Biomedical and Clinical Research, supported by the National Institute of Diabetes and Digestive and Kidney Diseases of the National Institutes of Health under Award Number R01DK115976 (JB). PH's research program also received research support during the project period from NIH grants DK-095980, HL-091333, HL-107256 and a Multi-campus grant from the University of California Office of the President.

Acknowledgments

The authors thank the technical support of Nishi Ivanov. In addition, the authors are appreciative of the efforts by Dr. Michael Schwartz and Dr. Dianne Lattemann for providing feedback throughout the course of these studies.

Conflict of interest

JB had a financial interest in OXT Therapeutics, Inc., a company developing highly specific and stable analogs of oxytocin to treat obesity and metabolic disease. The authors' interests were reviewed and are managed by their local institutions in accordance with their conflict of interest policies.

The remaining authors declare that the research was conducted in the absence of any commercial or financial relationships that could be construed as a potential conflict of interest.

The author(s) declared that they were an editorial board member of Frontiers, at the time of submission. This had no impact on the peer review process and the final decision.

Publisher's note

Author disclaimer

The content is solely the responsibility of the authors and does not necessarily represent the official views of the National Institutes of Health. The contents do not represent the views of the U.S. Department of Veterans Affairs or the United States Government.

Supplementary material

The Supplementary Material for this article can be found online at: https://www.frontiersin.org/articles/10.3389/fendo.2024.1440070/full#supplementary-material

SUPPLEMENTAL STUDY 1

Determine if surgical denervation of IBAT changes the ability of IP tyramine to increase T_{IBAT} in DIO mice. The goal of this study was to determine if IP tyramine-elicited increase in T_{IBAT} requires intact SNS outflow to IBAT in DIO mice. We selected doses of tyramine based on previous studies (105). By design, mice were DIO as determined by both body weight (49.5 ± 1.1 g) and adiposity (13.9 ± 0.8 g fat mass; 31.2 ± 1.4% adiposity) after maintenance on the HFD (60% kcal from fat; N=9-10/group) for approximately 4.25 months prior to sham/denervation procedures and implantation of temperature transponders underneath IBAT. Mice from Study 4 were used in this study and were otherwise treated identically to those used in Study 4. Supplemental Study 1. In sham mice, tyramine (6.4 mg/kg) increased T_{IBAT} at 0.25-h post-injection while the higher dose (19.2 mg/kg) increased T_{IBAT} at 0.25 and 0.5-h post-injection ($P<0.05$; Supplementary Figure 1A). The lower dose also reduced T_{IBAT} at 0.75, 1, 1.25, 1.75, and 3-h post-injection and tended to reduce T_{IBAT} at 2-h post-injection. The higher dose reduced T_{IBAT} at 1, 1.25 and 1.75-h post-injection. Similar findings were apparent when measuring change in T_{IBAT} relative to baseline T_{IBAT} (Supplementary Figure 1B). In denervated mice, tyramine (6.4 mg/kg) was not effective at increasing T_{IBAT} but tended to reduce T_{IBAT} at 0.75-h post-injection ($P<0.05$; Supplementary Figure 1C). The higher dose (19.2 mg/kg) stimulated T_{IBAT} at 0.25 and 0.5-h post-injection and reduced T_{IBAT} at 1.25, 1.5, 1.75 and 2-h post-injection ($P<0.05$). Similar findings were also apparent when measuring change in T_{IBAT} relative to baseline T_{IBAT} (Supplementary Figure 1D).

SUPPLEMENTAL STUDY 2

Determine if surgical denervation of IBAT changes the ability of 4V OT to increase T_{IBAT} in lean mice. The goal of this study was to determine if OT- elicited increase in T_{IBAT} requires intact SNS outflow to IBAT in lean mice. By design, mice were lean as determined by both body weight (29.5 ± 0.7 g) and adiposity (3.3 ± 0.3 g fat mass; 10.4 ± 0.8% adiposity) after maintenance on the chow (16% kcal from fat; N=10/group) for approximately 4-4.25 months prior to sham/denervation procedures and implantation of temperature transponders underneath IBAT. Mice were otherwise treated identically to those used in Study 4. Supplemental Study 2. Only a subset of samples from Study 1B were able to be screened for NE content but all mice were otherwise included in the analysis. In sham mice, 4V OT (5 μg/μL) increased T_{IBAT} at 0.5, 0.75, 1 and 3-h post-injection ($P<0.05$; Suplemental Figure 2A) and tended to stimulate T_{IBAT} at 0.75 (1 μg/μL) and 1.25 (5 μg/μL) h-post-injection. In addition, we found similar findings were apparent when measuring change in T_{IBAT} relative to baseline T_{IBAT} (Supplementary Figure 2B). Similarly, in denervated mice, 4V OT (5 μg/μL) increased T_{IBAT} at 0.75, 1, 1.25 and 3-h post-injection ($P<0.05$; Supplementary Figure 2C) and tended

to stimulate T_{IBAT} at 1.25 (1 μg/μL) -h post-injection. In contrast, 4V OT was unable to stimulate a change in T_{IBAT} relative to baseline T_{IBAT} (Supplementary Figure 2D).

SUPPLEMENTAL STUDY 3

Determine if a centrally (4V) effective dose of OT can increase T_{IBAT} when given into the periphery of lean mice. The goal of this study was to determine if systemic administration of OT (IP) can increase T_{IBAT} at a dose that was effective when given into the 4V in lean mice. By design, mice were lean (31.2 ± 0.8 g) at study onset after maintenance on the chow (16% kcal from fat; N=10/group) for approximately 5 months. Mice did not undergo sham or SNS IBAT denervation procedures but were implanted with temperature transponders underneath IBAT and were otherwise treated similarly to those used in Study 4.Supplemental Study 3. In contrast to the more immediate elevation of T_{IBAT} in response to 4V OT (5 μg/μL), IP OT (5 μg/0.200 mL) resulted in a reduction of T_{IBAT} at 0.25-h post-injection followed by increases in T_{IBAT} at 1.25 and 3-h post-injection ($P<0.05$; Supplementary Figure 3A). IP OT (5 μg/0.200 mL) also tended to stimulate T_{IBAT} at 1.25, 2 and 4-h post-injection. In addition, we found similar findings were apparent when measuring change in T_{IBAT} relative to baseline T_{IBAT} (Supplementary Figure 3B). In addition, a higher dose of OT (10 μg/0.200 mL) produced a similar reduction of T_{IBAT} at 15-min post-injection followed by increases in T_{IBAT} at 1.25, 1.5, 2, and 3-h post-injection ($P<0.05$; Supplementary Figure 3A). IP OT (10 μg/0.200 mL) also tended to stimulate T_{IBAT} at 105 min-post-injection. In addition, we found similar findings were apparent when measuring change in T_{IBAT} relative to baseline T_{IBAT} (Supplementary Figure 3B).

SUPPLEMENTARY FIGURE 1

(A-D). Effect of IP Tyramine on IBAT temperature (T_{IBAT}) in DIO mice (0927.23F). Mice were fed *ad libitum* and maintained on HFD (N=9-10/group) for 4.25 months prior to underdoing sham or SNS denervation procedures and implantation of temperature transponders underneath the left IBAT depot. Mice were allowed to recover for at least 1 week during which time they were adapted to a daily 4-h fast, handling and mock injections. Following completion of Supplemental Study 5, mice subsequently received IP injections (1.5 mL/kg; ≈ 0.07-0.09 mL/mouse) of tyramine (6.4 and 19.4 mg/kg) or vehicle (DMSO) where each animal received each treatment at least 48-h intervals. **(A, C)**, Effect of tyramine on T_{IBAT} in **(A)** sham operated or **(C)** IBAT denervated lean mice; **(B, D)**, Effect of tyramine on change in T_{IBAT} relative to baseline $T_{IBA}T$ (delta T_{IBAT}) in **(B)** sham operated or **(D)** IBAT denervated DIO mice. Data are expressed as mean ± SEM. $^*P<0.05$, $^\dagger 0.05<P<0.1$ tyramine vs. vehicle.

SUPPLEMENTARY FIGURE 2

(A-D) Effect of 4V OT on IBAT temperature (T_{IBAT}) post-sham or IBAT denervation in lean mice. Mice were maintained on chow (16% kcal from fat; N=10/group) for approximately for approximately 4-4.25 months prior to undergoing a sham or bilateral surgical IBAT denervation and implantation of temperature transponders underneath IBAT. Mice were subsequently implanted with 4V cannulas and allowed to recover for 3-4 weeks prior to receiving 4V injections of OT (1 or 5 μg/μL) or vehicle (sterile water) where each animal received each treatment at approximately 48-h intervals. *A/C*, Effect of OT on T_{IBAT} in **(A)** sham operated or **(C)** IBAT denervated lean mice; **(B, D)**, Effect of OT on change in T_{IBAT} relative to baseline $T_{IBA}T$ (delta T_{IBAT}) in **(B)** sham operated or **(D)** IBAT denervated lean mice. Data are expressed as mean ± SEM. $^*P<0.05$, $^\dagger 0.05<P<0.1$ OT vs. vehicle.

SUPPLEMENTARY FIGURE 3

(A-D) Effect of IP OT on IBAT temperature (T_{IBAT}) in lean mice. Mice were maintained on chow (16% kcal from fat; N=9-10/group) for approximately for approximately 2.5 months prior to implantation of temperature transponders underneath IBAT. Mice were subsequently implanted with 4V cannulas and allowed to recover for approximately 2 weeks prior to receiving acute 4V injections of OT or vehicle [data previously published (22)]. Mice subsequently received IP injections of OT (5 μg/0.200 μL or 10 μg/0.200 μL) or vehicle (sterile water) where each animal received each treatment at approximately 48-h intervals. **(A, C)**, Effect of **(A)** lower and **(C)** higher dose of IP OT on T_{IBAT} in lean mice; **(B, D)**, Effect of **(B)** lower and **(D)** higher dose of IP OT on change in T_{IBAT} relative to baseline $T_{IBA}T$ (delta T_{IBAT}) in lean mice. Data are expressed as mean ± SEM. $^*P<0.05$, $^\dagger 0.05<P<0.1$ OT vs. vehicle.

References

1. Gimpl G, Fahrenholz F. The oxytocin receptor system: structure, function, and regulation. *Physiol Rev*. (2001) 81:629–83. doi: 10.1152/physrev.2001.81.2.629

2. Kosfeld M, Heinrichs M, Zak PJ, Fischbacher U, Fehr E. Oxytocin increases trust in humans. *Nature*. (2005) 435:673–6. doi: 10.1038/nature03701

3. Striepens N, Kendrick KM, Maier W, Hurlemann R. Prosocial effects of oxytocin and clinical evidence for its therapeutic potential. *Front Neuroendocrinol*. (2011) 32:426–50. doi: 10.1016/j.yfrne.2011.07.001

4. Blevins JE, Baskin DG. Translational and therapeutic potential of oxytocin as an anti-obesity strategy: Insights from rodents, nonhuman primates and humans. *Physiol Behav*. (2015) 152(Pt B):438–49. doi: 10.1016/j.physbeh.2015.05.023

5. Lawson EA. The effects of oxytocin on eating behaviour and metabolism in humans. *Nat Rev Endocrinol*. (2017) 13:700–9. doi: 10.1038/nrendo.2017.115

6. Lawson EA, Olszewski PK, Weller A, Blevins JE. The role of oxytocin in regulation of appetitive behaviour, body weight and glucose homeostasis. *J Neuroendocrinol*. (2020) 32:e12805. doi: 10.1111/jne.12805

7. McCormack SE, Blevins JE, Lawson EA. Metabolic effects of oxytocin. *Endocrine Rev*. (2020) 41:121–45. doi: 10.1210/endrev/bnz012

8. Altirriba J, Poher AL, Rohner-Jeanrenaud F. Chronic oxytocin administration as a treatment against impaired leptin signaling or leptin resistance in obesity. *Front Endocrinol*. (2015) 6:119. doi: 10.3389/fendo.2015.00119

9. Deblon N, Veyrat-Durebex C, Bourgoin L, Caillon A, Bussier AL, Petrosino S, et al. Mechanisms of the anti-obesity effects of oxytocin in diet-induced obese rats. *PloS One*. (2011) 6:e25565. doi: 10.1371/journal.pone.0025565

10. Morton GJ, Thatcher BS, Reidelberger RD, Ogimoto K, Wolden-Hanson T, Baskin DG, et al. Peripheral oxytocin suppresses food intake and causes weight loss in diet-induced obese rats. *Am J Physiol-Endoc M*. (2012) 302:E134–44. doi: 10.1152/ajpendo.00296.2011

11. Blevins JE, Graham JL, Morton GJ, Bales KL, Schwartz MW, Baskin DG, et al. Chronic oxytocin administration inhibits food intake, increases energy expenditure, and produces weight loss in fructose-fed obese rhesus monkeys. *Am J Physiol Regul Integr Comp Physiol*. (2015) 308:R431–8. doi: 10.1152/ajpregu.00441.2014

12. Noble EE, Billington CJ, Kotz CM, Wang C. Oxytocin in the ventromedial hypothalamic nucleus reduces feeding and acutely increases energy expenditure. *Am J Physiol Regul Integr Comp Physiol*. (2014) 307:R737–45. doi: 10.1152/ajpregu.00118.2014

13. Zhang G, Bai H, Zhang H, Dean C, Wu Q, Li J, et al. Neuropeptide exocytosis involving synaptotagmin-4 and oxytocin in hypothalamic programming of body weight and energy balance. *Neuron*. (2011) 69:523–35. doi: 10.1016/j.neuron.2010.12.036

14. Zhang G, Cai D. Circadian intervention of obesity development via resting-stage feeding manipulation or oxytocin treatment. *Am J Physiol Endocrinol Metab*. (2011) 301:E1004–12. doi: 10.1152/ajpendo.00196.2011

15. Cannon B, Nedergaard J. Brown adipose tissue: function and physiological significance. *Physiol Rev*. (2004) 84:277–359. doi: 10.1152/physrev.00015.2003

16. Morrison SF, Madden CJ, Tupone D. Central neural regulation of brown adipose tissue thermogenesis and energy expenditure. *Cell Metab*. (2014) 19:741–56. doi: 10.1016/j.cmet.2014.02.007

17. Kotz CM, Perez-Leighton CE, Teske JA, Billington CJ. Spontaneous physical activity defends against obesity. *Curr Obes Rep*. (2017) 6:362–70. doi: 10.1007/s13679-017-0288-1

18. Periasamy M, Herrera JL, Reis FCG. Skeletal muscle thermogenesis and its role in whole body energy metabolism. *Diabetes Metab J*. (2017) 41:327–36. doi: 10.4093/dmj.2017.41.5.327

19. Cereijo R, Villarroya J, Villarroya F. Non-sympathetic control of brown adipose tissue. *Int J Obes Supplments*. (2015) 5:S40–4. doi: 10.1038/ijosup.2015.10

20. Lopez M, Alvarez CV, Nogueiras R, Dieguez C. Energy balance regulation by thyroid hormones at central level. *Trends Mol Med*. (2013) 19:418–27. doi: 10.1016/j.molmed.2013.04.004

21. Roberts ZS, Wolden-Hanson TH, Matsen ME, Ryu V, Vaughan CH, Graham JL, et al. Chronic hindbrain administration of oxytocin is sufficient to elicit weight loss in diet-induced obese rats. *Am J Physiol Regul Integr Comp Physiol*. (2017) 313(4):R357–71. doi: 10.1152/ajpregu.00169.2017

22. Edwards MM, Nguyen HK, Herbertson AJ, Dodson AD, Wietecha T, Wolden-Hanson T, et al. Chronic hindbrain administration of oxytocin elicits weight loss in male diet-induced obese mice. *Am J Physiol Regul Integr Comp Physiol*. (2021) 320(4):R471–87. doi: 10.1152/ajpregu.00294.2020

23. Sutton AK, Pei H, Burnett KH, Myers MG Jr., Rhodes CJ, Olson DP. Control of food intake and energy expenditure by Nos1 neurons of the paraventricular hypothalamus. *J Neurosci*. (2014) 34:15306–18. doi: 10.1523/JNEUROSCI.0226-14.2014

24. Yuan J, Zhang R, Wu R, Gu Y, Lu Y. The effects of oxytocin to rectify metabolic dysfunction in obese mice are associated with increased thermogenesis. *Mol Cell Endocrinol*. (2020) 514:110903. doi: 10.1016/j.mce.2020.110903

25. Camerino C. Low sympathetic tone and obese phenotype in oxytocin-deficient mice. *Obesity*. (2009) 17:980–4. doi: 10.1038/oby.2009.12

26. Takayanagi Y, Kasahara Y, Onaka T, Takahashi N, Kawada T, Nishimori K. Oxytocin receptor-deficient mice developed late-onset obesity. *Neuroreport*. (2008) 19:951–5. doi: 10.1097/WNR.0b013e3283021ca9

27. Wu Z, Xu Y, Zhu Y, Sutton AK, Zhao R, Lowell BB, et al. An obligate role of oxytocin neurons in diet induced energy expenditure. *PloS One*. (2012) 7:e45167. doi: 10.1371/journal.pone.0045167

28. Kasahara Y, Sato K, Takayanagi Y, Mizukami H, Ozawa K, Hidema S, et al. Oxytocin receptor in the hypothalamus is sufficient to rescue normal thermoregulatory function in male oxytocin receptor knockout mice. *Endocrinology*. (2013) 154:4305–15. doi: 10.1210/en.2012-2206

29. Kasahara Y, Tateishi Y, Hiraoka Y, Otsuka A, Mizukami H, Ozawa K, et al. Role of the oxytocin receptor expressed in the rostral medullary raphe in thermoregulation during cold conditions. *Front Endocrinol*. (2015) 6:180. doi: 10.3389/fendo.2015.00180

30. Harshaw C, Leffel JK, Alberts JR. Oxytocin and the warm outer glow: Thermoregulatory deficits cause huddling abnormalities in oxytocin-deficient mouse pups. *Hormones Behav*. (2018) 98:145–58. doi: 10.1016/j.yhbeh.2017.12.007

31. Xi D, Long C, Lai M, Casella A, O'Lear L, Kublaoui B, et al. Ablation of oxytocin neurons causes a deficit in cold stress response. *J Endocrine Soc*. (2017) 1:1041–55. doi: 10.1210/js.2017-00136

32. Thureson-Klein A, Mill-Hyde B, Barnard T, Lagercrantz H. Ultrastructrual effects of chemical sympathectomy on brown adipose tissue. *J Neurocytol*. (1976) 5:677–90. doi: 10.1007/BF01181581

33. Depocas F, Foster DO, Zaror-Behrens G, Lacelle S, Nadeau B. Recovery of function in sympathetic nerves of interscapular brown adipose tissue of rats treated with 6-hydroxydopamine. *Can J Physiol Pharmacol*. (1984) 62:1327–32. doi: 10.1139/y84-222

34. Wang LY, Murphy RR, Hanscom B, Li G, Millard SP, Petrie EC, et al. Cerebrospinal fluid norepinephrine and cognition in subjects across the adult age span. *Neurobiol Aging*. (2013) 34:2287–92. doi: 10.1016/j.neurobiolaging.2013.04.007

35. Williams DL, Bowers RR, Bartness TJ, Kaplan JM, Grill HJ. Brainstem melanocortin 3/4 receptor stimulation increases uncoupling protein gene expression in brown fat. *Endocrinology*. (2003) 144:4692–7. doi: 10.1210/en.2003-0440

36. De Boer SF, van der Gugten J. Daily variations in plasma noradrenaline. *Adrenaline Corticosterone Concentrations Rats Physiol Behav*. (1987) 40:323–8. doi: 10.1016/0031-9384(87)90054-0

37. Davidovic V, Petrovic VM. Diurnal variations in the catecholamine content in rat tissues Effects of exogenous noradrenaline. *Arch Iniernationales Physiologie Biochimie*. (1981) 89:457–60. doi: 10.3109/13813458109082642

38. Suarez J, Rivera P, Arrabal S, Crespillo A, Serrano A, Baixeras E, et al. Oleoylethanolamide enhances beta-adrenergic-mediated thermogenesis and white-to-brown adipocyte phenotype in epididymal white adipose tissue in rat. *Dis Models Mech*. (2014) 7:129–41. doi: 10.1242/dmm.013110

39. Malinowska B, Schlicker E. Further evidence for differences between cardiac atypical beta-adrenoceptors and brown adipose tissue beta3-adrenoceptors in the pithed rat. *Br J Pharmacol*. (1997) 122:1307–14. doi: 10.1038/sj.bjp.0701516

40. Lateef DM, Abreu-Vieira G, Xiao C, Reitman ML. Regulation of body temperature and brown adipose tissue thermogenesis by bombesin receptor subtype-3. *Am J Physiol Endocrinol Metab*. (2014) 306:E681–7. doi: 10.1152/ajpendo.00615.2013

41. Ma S, Yu H, Zhao Z, Luo Z, Chen J, Ni Y, et al. Activation of the cold-sensing TRPM8 channel triggers UCP1-dependent thermogenesis and prevents obesity. *J Mol Cell Biol*. (2012) 4:88–96. doi: 10.1093/jmcb/mjs001

42. Liskiewicz D, Zhang Q, Barthem CS, Jastroch M, Liskiewicz A, Khajavi N, et al. Neuronal loss of TRPM8 leads to obesity and glucose intolerance in male mice. *Mol Metab*. (2023) 72:101714. doi: 10.1016/j.molmet.2023.101714

43. Modi ME, Inoue K, Barrett CE, Kittelberger KA, Smith DG, Landgraf R, et al. Melanocortin receptor agonists facilitate oxytocin-dependent partner preference formation in the prairie vole. *Neuropsychopharmacology: Off Publ Am Coll Neuropsychopharmacol*. (2015) 40:1856–65. doi: 10.1038/npp.2015.35

44. Olszewski PK, Wirth MM, Shaw TJ, Grace MK, Billington CJ, Giraudo SQ, et al. Role of alpha-MSH in the regulation of consummatory behavior: immunohistochemical evidence. *Am J Physiol Regul Integr Comp Physiol*. (2001) 281: R673–80. doi: 10.1152/ajpregu.2001.281.2.R673

45. Semple E, Shalabi F, Hill JW. Oxytocin neurons enable melanocortin regulation of male sexual function in mice. *Mol Neurobiol*. (2019) 56:6310–23. doi: 10.1007/s12035-019-1514-5

46. Blevins JE, Thompson BW, Anekonda VT, Ho JM, Graham JL, Roberts ZS, et al. Chronic CNS oxytocin signaling preferentially induces fat loss in high fat diet-fed rats by enhancing satiety responses and increasing lipid utilization. *Am J Physiol-Reg I*. (2016) 310(7):R640–58. doi: 10.1152/ajpregu.00220.2015

47. Bremer AA, Stanhope KL, Graham JL, Cummings BP, Wang W, Saville BR, et al. Fructose-fed rhesus monkeys: a nonhuman primate model of insulin resistance, metabolic syndrome, and type 2 diabetes. *Clin Trans Sci*. (2011) 4:243–52. doi: 10.1111/cts.2011.4.issue-4

48. Blevins JE, Moralejo DH, Wolden-Hanson TH, Thatcher BS, Ho JM, Kaiyala KJ, et al. Alterations in activity and energy expenditure contribute to lean phenotype in Fischer 344 rats lacking the cholecystokinin-1 receptor gene. *Am J Physiol Regul Integr Comp Physiol*. (2012) 303:R1231–40. doi: 10.1152/ajpregu.00393.2012

49. Cummings BP, Digitale EK, Stanhope KL, Graham JL, Baskin DG, Reed BJ, et al. Development and characterization of a novel rat model of type 2 diabetes mellitus: the UC Davis type 2 diabetes mellitus UCD-T2DM rat. *Am J Physiol Regul Integr Comp Physiol*. (2008) 295:R1782–93. doi: 10.1152/ajpregu.90635.2008

50. Livak KJ, Schmittgen TD. Analysis of relative gene expression data using real-time quantitative PCR and the 2(-Delta Delta C(T)) Method. *Methods*. (2001) 25:402–8. doi: 10.1006/meth.2001.1262

51. Nguyen NL, Barr CL, Ryu V, Cao Q, Xue B, Bartness TJ. Separate and shared sympathetic outflow to white and brown fat coordinately regulate thermoregulation and beige adipocyte recruitment. *Am J Physiol Regul Integr Comp Physiol*. (2016) 312 (1):R132–45. doi: 10.1152/ajpregu.00344.2016

52. Cao Q, Jing J, Cui X, Shi H, Xue B. Sympathetic nerve innervation is required for beigeing in white fat. *Physiol Rep*. (2019) 7:e14031. doi: 10.14814/phy2.14031

53. Klingenspor M, Meywirth A, Stohr S, Heldmaier G. Effect of unilateral surgical denervation of brown adipose tissue on uncoupling protein mRNA level and cytochrom-c-oxidase activity in the Djungarian hamster. *J Comp Physiol B*. (1994) 163:664–70. doi: 10.1007/BF00369517

54. Fischer AW, Schlein C, Cannon B, Heeren J, Nedergaard J. Intact innervation is essential for diet-induced recruitment of brown adipose tissue. *Am J Physiol Endocrinol Metab*. (2019) 316:E487–503. doi: 10.1152/ajpendo.00443.2018

55. Bajzer M, Olivieri M, Haas MK, Pfluger PT, Magrisso IJ, Foster MT, et al. Cannabinoid receptor 1 (CB1) antagonism enhances glucose utilisation and activates brown adipose tissue in diet-induced obese mice. *Diabetologia*. (2011) 54:3121–31. doi: 10.1007/s00125-011-2302-6

56. Labbe SM, Caron A, Festuccia WT, Lecomte R, Richard D. Interscapular brown adipose tissue denervation does not promote the oxidative activity of inguinal white adipose tissue in male mice. *Am J Physiol Endocrinol Metab*. (2018) 315:E815–24. doi: 10.1152/ajpendo.00210.2018

57. Bahler L, Verberne HJ, Admiraal WM, Stok WJ, Soeters MR, Hoekstra JB, et al. Differences in sympathetic nervous stimulation of brown adipose tissue between the young and old, and the lean and obese. *J Nucl medicine: Off publication Soc Nucl Med*. (2016) 57:372–7. doi: 10.2967/jnumed.115.165829

58. Zoico E, Rubele S, De Caro A, Nori N, Mazzali G, Fantin F, et al. Brown and beige adipose tissue and aging. *Front Endocrinol*. (2019) 10:368. doi: 10.3389/fendo.2019.00368

59. Doslikova B, Tchir D, McKinty A, Zhu X, Marks DL, Baracos VE, et al. Convergent neuronal projections from paraventricular nucleus, parabrachial nucleus, and brainstem onto gastrocnemius muscle, white and brown adipose tissue in male rats. *J Comp Neurol*. (2019) 527:2826–42. doi: 10.1002/cne.24710

60. Oldfield BJ, Giles ME, Watson A, Anderson C, Colvill LM, McKinley MJ. The neurochemical characterisation of hypothalamic pathways projecting polysynaptically to brown adipose tissue in the rat. *Neuroscience*. (2002) 110:515–26. doi: 10.1016/S0306-4522(01)00555-3

61. Shi H, Bartness TJ. Neurochemical phenotype of sympathetic nervous system outflow from brain to white fat. *Brain Res Bull*. (2001) 54:375–85. doi: 10.1016/S0361-9230(00)00455-X

62. Stanley S, Pinto S, Segal J, Perez CA, Viale A, DeFalco J, et al. Identification of neuronal subpopulations that project from hypothalamus to both liver and adipose tissue polysynaptically. *Proc Natl Acad Sci U.S.A*. (2010) 107:7024–9. doi: 10.1073/pnas.1002790107

63. Rinaman L. Oxytocinergic inputs to the nucleus of the solitary tract and dorsal motor nucleus of the vagus in neonatal rats. *J Comp Neurol*. (1998) 399:101–9. doi: 10.1002/(ISSN)1096-9861

64. Sawchenko PE, Swanson LW. Immunohistochemical identification of neurons in the paraventricular nucleus of the hypothalamus that project to the medulla or to the spinal cord in the rat. *J Comp Neurol*. (1982) 205:260–72. doi: 10.1002/cne.902050306

65. Bamshad M, Song CK, Bartness TJ. CNS origins of the sympathetic nervous system outflow to brown adipose tissue. *Am J Physiol*. (1999) 276:R1569–78. doi: 10.1152/ajpregu.1999.276.6.R1569

66. Cano G, Passerin AM, Schiltz JC, Card JP, Morrison SF, Sved AF. Anatomical substrates for the central control of sympathetic outflow to interscapular adipose tissue during cold exposure. *J Comp Neurol*. (2003) 460:303–26. doi: 10.1002/cne.10643

67. Ong ZY, Bongiorno DM, Hernando MA, Grill HJ. Effects of endogenous oxytocin receptor signaling in nucleus tractus solitarius on satiation-mediated feeding and thermogenic control in male rats. *Endocrinology*. (2017) 158:2826–36. doi: 10.1210/en.2017-00200

68. Kong D, Tong Q, Ye C, Koda S, Fuller PM, Krashes MJ, et al. GABAergic RIP-Cre neurons in the arcuate nucleus selectively regulate energy expenditure. *Cell*. (2012) 151:645–57. doi: 10.1016/j.cell.2012.09.020

69. Morrison SF, Nakamura K. Central neural pathways for thermoregulation. *Front bioscience*. (2011) 16:74–104. doi: 10.2741/3677

70. Morrison SF. Central control of body temperature. *F1000Research*. (2016) 5. doi: 10.12688/f1000research

71. Reed N, Fain JN. Stimulation of respiration in brown fat cells by epinephrine, dibutyryl-3',5'-adenosine monophosphate, and m-chloro(carbonyl cyanide) phenylhydrazone. *J Biol Chem*. (1968) 243:2843–8. doi: 10.1016/S0021-9258(18)93348-X

72. Strosberg AD. Structure and function of the beta 3-adrenergic receptor. *Annu Rev Pharmacol Toxicol*. (1997) 37:421–50. doi: 10.1146/annurev.pharmtox.37.1.421

73. Sharara-Chami RI, Joachim M, Mulcahey M, Ebert S, Majzoub JA. Effect of epinephrine deficiency on cold tolerance and on brown adipose tissue. *Mol Cell Endocrinol*. (2010) 328:34–9. doi: 10.1016/j.mce.2010.06.019

74. Strack AM, Sawyer WB, Platt KB, Loewy AD. CNS cell groups regulating the sympathetic outflow to adrenal gland as revealed by transneuronal cell body labeling with pseudorabies virus. *Brain Res*. (1989) 491:274–96. doi: 10.1016/0006-8993(89)90063-2

75. Dum RP, Levinthal DJ, Strick PL. The mind-body problem: Circuits that link the cerebral cortex to the adrenal medulla. *Proc Natl Acad Sci U.S.A*. (2019) 116:26321–8. doi: 10.1073/pnas.1902297116

76. Sakamoto T, Sugimoto S, Uekita T. Effects of intraperitoneal and intracerebroventricular injections of oxytocin on social and emotional behaviors in pubertal male mice. *Physiol Behav*. (2019) 212:112701. doi: 10.1016/j.physbeh.2019.112701

77. Asker M, Krieger JP, Liles A, Tinsley IC, Borner T, Maric I, et al. Peripherally restricted oxytocin is sufficient to reduce food intake and motivation, while CNS entry is required for locomotor and taste avoidance effects. *Diabetes Obes Metab*. (2023) 25:856–77. doi: 10.1111/dom.14937

78. Iwasaki Y, Kumari P, Wang L, Hidema S, Nishimori K, Yada T. Relay of peripheral oxytocin to central oxytocin neurons via vagal afferents for regulating feeding. *Biochem Biophys Res Commun*. (2019) 519:553–8. doi: 10.1016/j.bbrc.2019.09.039

79. Iwasaki Y, Maejima Y, Suyama S, Yoshida M, Arai T, Katsurada K, et al. Peripheral oxytocin activates vagal afferent neurons to suppress feeding in normal and leptin-resistant mice: a route for ameliorating hyperphagia and obesity. *Am J Physiol Regul Integr Comp Physiol*. (2015) 308:R360–9. doi: 10.1152/ajpregu.00344.2014

80. Ho JM, Anekonda VT, Thompson BW, Zhu M, Curry RW, Hwang BH, et al. Hindbrain oxytocin receptors contribute to the effects of circulating oxytocin on food intake in male rats. *Endocrinology*. (2014) 155:2845–57. doi: 10.1210/en.2014-1148

81. Schaffler A, Binart N, Scholmerich J, Buchler C. Hypothesis paper Brain talks with fat–evidence for a hypothalamic-pituitary-adipose axis? *Neuropeptides*. (2005) 39:363–7. doi: 10.1016/j.npep.2005.06.003

82. Yi KJ, So KH, Hata Y, Suzuki Y, Kato D, Watanabe K, et al. The regulation of oxytocin receptor gene expression during adipogenesis. *J Neuroendocrinol*. (2015) 27:335–42. doi: 10.1111/jne.12268

83. Hicks C, Ramos L, Reekie T, Misagh GH, Narlawar R, Kassiou M, et al. Body temperature and cardiac changes induced by peripherally administered oxytocin, vasopressin and the non-peptide oxytocin receptor agonist WAY 267,464: a biotelemetry study in rats. *Br J Pharmacol*. (2014) 171:2868–87. doi: 10.1111/bph.12613

84. Ring RH, Malberg JE, Potestio L, Ping J, Boikess S, Luo B, et al. Anxiolytic-like activity of oxytocin in male mice: behavioral and autonomic evidence, therapeutic implications. *Psychopharmacology*. (2006) 185:218–25. doi: 10.1007/s00213-005-0293-z

85. Kohli S, King MV, Williams S, Edwards A, Ballard TM, Steward LJ, et al. Oxytocin attenuates phencyclidine hyperactivity and increases social interaction and nucleus accumben dopamine release in rats. *Neuropsychopharmacology: Off Publ Am Coll Neuropsychopharmacol*. (2019) 44:295–305. doi: 10.1038/s41386-018-0171-0

86. Xu Y, Kim ER, Fan S, Xia Y, Xu Y, Huang C, et al. Profound and rapid reduction in body temperature induced by the melanocortin receptor agonists. *Biochem Biophys Res Commun*. (2014) 451:184–9. doi: 10.1016/j.bbrc.2014.07.079

87. Lute B, Jou W, Lateef DM, Goldgof M, Xiao C, Pinol RA, et al. Biphasic effect of melanocortin agonists on metabolic rate and body temperature. *Cell Metab*. (2014) 20:333–45. doi: 10.1016/j.cmet.2014.05.021

88. Jain S, Panyutin A, Liu N, Xiao C, Pinol RA, Pundir P, et al. Melanotan II causes hypothermia in mice by activation of mast cells and stimulation of histamine 1 receptors. *Am J Physiol Endocrinol Metab*. (2018) 315:E357–66. doi: 10.1152/ajpendo.00024.2018

89. Blouquit MF, Koubi H, Geloen A, Gripois D. Norepinephrine content in the brown adipose tissue of the developing obese Zucker rat. *Hormone Metab Res = Hormon- und Stoffwechselforschung = Hormones metabolisme*. (1991) 23:239. doi: 10.1055/s-2007-1003662

90. Blouquit MF, Gripois D. Tyrosine hydroxylase activity in the brown adipose tissue of the obese Zucker rat during development. *Hormone Metab Res = Hormon- und Stoffwechselforschung = Hormones metabolisme*. (1990) 22:123. doi: 10.1055/s-2007-1004865

91. Blouquit MF, Geloen A, Koubi H, Edwards D, Gripois D. Decreased norepinephrine turnover rate in the brown adipose tissue of pre-obese fa/fa Zucker rats. *J Dev Physiol*. (1993) 19:247–51.

92. Leitner BP, Huang S, Brychta RJ, Duckworth CJ, Baskin AS, McGehee S, et al. Mapping of human brown adipose tissue in lean and obese young men. *Proc Natl Acad Sci U.S.A*. (2017) 114:8649–54. doi: 10.1073/pnas.1705287114

93. Vijgen GH, Bouvy ND, Teule GJ, Brans B, Schrauwen P, van Marken Lichtenbelt WD. Brown adipose tissue in morbidly obese subjects. *PloS One*. (2011) 6:e17247. doi: 10.1371/journal.pone.0017247

94. Valentine JM, Ahmadian M, Keinan O, Abu-Odeh M, Zhao P, Zhou X, et al. beta3-Adrenergic receptor downregulation leads to adipocyte catecholamine resistance in obesity. *J Clin Invest*. (2022) 132. doi: 10.1172/JCI153357

95. de Almeida DL, Fabricio GS, Trombini AB, Pavanello A, Tofolo LP, da Silva Ribeiro TA, et al. Early overfeed-induced obesity leads to brown adipose tissue hypoactivity in rats. *Cell Physiol Biochemistry: Int J Exp Cell Physiology Biochemistry Pharmacol*. (2013) 32:1621–30. doi: 10.1159/000356598

96. Lerea JS, Ring LE, Hassouna R, Chong AC, Szigeti-Buck K, Horvath TL, et al. Reducing adiposity in a critical developmental window has lasting benefits in mice. *Endocrinology*. (2016) 157:666–78. doi: 10.1210/en.2015-1753

97. Rangel-Azevedo C, Santana-Oliveira DA, Miranda CS, Martins FF, Mandarim-de-Lacerda CA, Souza-Mello V. Progressive brown adipocyte dysfunction: Whitening and impaired nonshivering thermogenesis as long-term obesity complications. *J Nutr Biochem*. (2022) 105:109002. doi: 10.1016/j.jnutbio.2022.109002

98. Edwards MM, Nguyen HK, Dodson AD, Herbertson AJ, Wietecha TA, Wolden-Hanson T, et al. Effects of combined oxytocin and beta-3 receptor agonist (CL 316243) treatment on body weight and adiposity in male diet-induced obese rats. *Front Physiol*. (2021) 12. doi: 10.3389/fphys.2021.725912

99. Baker JG. The selectivity of beta-adrenoceptor antagonists at the human beta1, beta2 and beta3 adrenoceptors. *Br J Pharmacol*. (2005) 144:317–22. doi: 10.1038/sj.bjp.0706048

100. Hutchinson DS, Chernogubova E, Sato M, Summers RJ, Bengtsson T. Agonist effects of zinterol at the mouse and human beta(3)-adrenoceptor. *Naunyn Schmiedebergs Arch Pharmacol*. (2006) 373:158–68. doi: 10.1007/s00210-006-0056-3

101. Susulic VS, Frederich RC, Lawitts J, Tozzo E, Kahn BB, Harper ME, et al. Targeted disruption of the beta 3-adrenergic receptor gene. *J Biol Chem*. (1995) 270:29483–92. doi: 10.1074/jbc.270.49.29483

102. Grujic D, Susulic VS, Harper ME, HimmsHagen J, Cunningham BA, Corkey BE, et al. beta 3-adrenergic receptors on white and brown adipocytes mediate beta 3-selective agonist-induced effects on energy expenditure, insulin secretion, and food intake - A study using transgenic and gene knockout mice. *J Biol Chem*. (1997) 272:17686–93. doi: 10.1074/jbc.272.28.17686

103. Ootsuka Y, Blessing WW, Nalivaiko E. Selective blockade of 5-HT2A receptors attenuates the increased temperature response in brown adipose tissue to restraint stress in rats. *Stress*. (2008) 11:125–33. doi: 10.1080/10253890701638303

104. Harris WH, Foster DO, Ma SW, Yamashiro S, Langlais-Burgess LA. The noradrenaline content and innervation of brown adipose tissue in the young rabbit. *Can J Physiol Pharmacol*. (1986) 64:561–7. doi: 10.1139/y86-093

105. Taborsky GJ Jr., Mei Q, Hackney DJ, Figlewicz DP, LeBoeuf R, Mundinger TO. Loss of islet sympathetic nerves and impairment of glucagon secretion in the NOD mouse: relationship to invasive insulitis. *Diabetologia*. (2009) 52:2602–11. doi: 10.1007/s00125-009-1494-5

106. Gilliam LK, Palmer JP, Taborsky GJ Jr. Tyramine-mediated activation of sympathetic nerves inhibits insulin secretion in humans. *J Clin Endocrinol Metab*. (2007) 92:4035–8. doi: 10.1210/jc.2007-0536

107. Bartness TJ, Vaughan CH, Song CK. Sympathetic and sensory innervation of brown adipose tissue. *Int J Obes (Lond)*. (2010) 34 Suppl 1:S36–42. doi: 10.1038/ijo.2010.182

108. Bal NC, Maurya SK, Singh S, Wehrens XH, Periasamy M. Increased reliance on muscle-based thermogenesis upon acute minimization of brown adipose tissue function. *J Biol Chem*. (2016) 291:17247–57. doi: 10.1074/jbc.M116.728188

109. de Jong JM, Larsson O, Cannon B, Nedergaard J. A stringent validation of mouse adipose tissue identity markers. *Am J Physiol Endocrinol Metab*. (2015) 308:E1085–105. doi: 10.1152/ajpendo.00023.2015